HHS Public Access

Author manuscript

Biochem Pharmacol. Author manuscript; available in PMC 2021 October 01.

Published in final edited form as:

Biochem Pharmacol. 2020 October ; 180: 114187. doi:10.1016/j.bcp.2020.114187.

Brain uptake pharmacokinetics of incretin receptor agonists showing promise as Alzheimer's and Parkinson's disease therapeutics

Therese S. Salameh[a], **Elizabeth M. Rhea**[a], **Konrad Talbot**[b], **William A. Banks**[a,*]

[a]Veterans Affairs Puget Sound Health Care System, Geriatrics Research Education and Clinical Center and University of Washington School of Medicine, Division of Gerontology and Geriatric Medicine, Department of Medicine, Seattle WA, USA 98498

[b]Loma Linda University School of Medicine, Departments of Neurosurgery, Basic Sciences, and Pathology and Human Anatomy, Loma Linda, CA, USA 92354

Abstract

Among the more promising treatments proposed for Alzheimer's disease (AD) and Parkinson's disease (PD) are those reducing brain insulin resistance. The antidiabetics in the class of incretin receptor agonists (IRAs) reduce symptoms and brain pathology in animal models of AD and PD, as well as glucose utilization in AD cases and clinical symptoms in PD cases after their systemic administration. At least 9 different IRAs are showing promise as AD and PD therapeutics, but we still lack quantitative data on their relative ability to cross the blood-brain barrier (BBB) reaching the brain parenchyma. We consequently compared brain uptake pharmacokinetics of intravenous ^{125}I-labeled IRAs in adult CD-1 mice over the course of 60 min. We tested single IRAs (exendin-4, liraglutide, lixisenatide, and semaglutide), which bind receptors for one incretin (glucagon-like peptide-1 [GLP-1]), and dual IRAs, which bind receptors for two incretins (GLP-1 and glucose-dependent insulinotropic polypeptide [GIP]), including unbranched, acylated, PEGylated, or C-terminally modified forms (Finan/Ma Peptides 17, 18, and 20 and Hölscher peptides DA3-CH and DA-JC4). The non-acylated and non-PEGylated IRAs (exendin-4, lixisenatide, Peptide 17, DA3-CH and DA-JC4) had significant rates of blood-to-brain influx (K*i*), but the acylated IRAs (liraglutide, semaglutide, and Peptide 18) did not measurably cross the BBB. The brain influx of the non-acylated, non-PEGylated IRAs were not saturable up to 1 μg of

*Correspondence Author: wabanks1@uw.edu.

CRediT authorship contribution statement

Therese S. Salameh: Project administration, investigation, data curation, formal analysis, visualization, writing - original draft, and funding (NIH grant RO1AG046619). **Elizabeth M. Rhea:** Investigation, formal analysis, writing - original draft, and funding (NIH grant T32AG000057). **Konrad Talbot:** Conceptualization, resources, visualization, writing - reviewing and editing, and funding (NIH grant RO1AG057658). **William A. Banks:** Supervision, methodology, resources, writing – reviewing and editing, and funding (NIH grant RO1AG046619).

Declaration of interest: none

Conflic of Interest

The authors report no conflict of interest.

these drugs and was most likely mediated by adsorptive transcytosis across brain endothelial cells, as observed for exendin-4. Of the non-acylated, non-PEGylated IRAs tested, exendin-4 and DA-JC4 were best able to cross the BBB based on their rate of brain influx, percentage reaching the brain that accumulated in brain parenchyma, and percentage of the systemic dose taken up per gram of brain tissue. Exendin-4 and DA-JC4 thus merit special attention as IRAs well-suited to enter the central nervous system (CNS), thus reaching areas pathologic in AD and PD.

Graphical Abstract

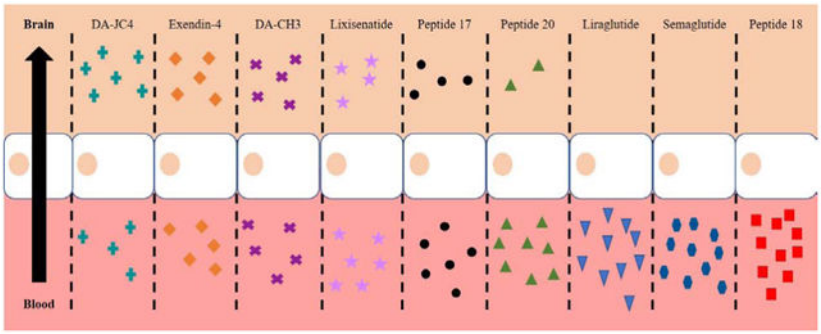

Keywords

Alzheimer’s disease; blood-brain barrier; incretin receptor agonists; Parkinson’s disease; pharmacokinetics

1. Introduction

Alzheimer’s disease (AD) and Parkinson’s disease (PD) are the two most common neurodegenerative disorders [1, 2]. We lack clinically effective treatments for both diseases. While several drugs have been FDA approved for symptomatic improvement of AD [3], all clinically-tested drugs for the disease have failed to produce significant improvements in cognition (i.e., increase of at least 3 points on the mini-mental state examination [MMSE]) [4] or to slow disease progression [4-8]. Similarly, all clinically-tested drugs for PD, while providing symptomatic relief early in the disorder, fail to slow its progression [9-11] and can, in the case of common dopaminergic treatments, induce motor and non-motor complications causing greater treatment-resistant disability later in the disorder [10-12]. In the absence of clinically effective treatments, AD and PD impose major economic burdens on our healthcare system [3, 13] and continue to exert tragic costs on patients and their families.

1.1. Insulin resistance as a promising therapeutic target in AD and PD

Given the noted deficiencies of drugs approved or proposed for treatment of AD and PD, most of which target only limited and conventional causal factors in these disorders (e.g., Aβ elevation in AD and dopamine dysregulation in PD), many investigators are now exploring novel causal factors in these disorders as targets for improvements. One of the novel factors is insulin resistance. Systemic insulin resistance is common in AD [14-17] and in PD [15,

16, 18]. Brain insulin resistance, which can be induced by systemic insulin resistance [19-23] or independently by brain Aβ oligomers and hyperphosphorylated tau [24], promotes many AD-like [22, 25-27] and PD-like [16, 28, 29] pathologies.

Systemic and especially brain insulin resistance are thus efficient targets for new treatments of AD [27, 30, 31] and PD [28, 29, 31]. Among the most promising drugs being tested are the antidiabetics known as incretin receptor agonists (IRAs). These drugs are effective in reducing systemic insulin resistance independent of weight loss in obesity and type 2 diabetes (T2D) [32-34] and in reducing brain insulin resistance in AD [35] and PD [36], which may explain their potent neuroprotective effects in animal models of AD [37-50] and PD [51-63]. The promise IRAs have shown in animal model studies has been validated by clinical trials showing that such drugs positively impact brain glucose uptake [36] and cerebral glucose utilization [64] in AD and alleviate clinical symptoms in PD [65-68].

1.2. The diversity of antidiabetic IRAs showing potential as AD and PD therapeutics

Many different IRAs have been introduced, originally for the purpose of treating T2D based on the discovery that incretin hormones increase glucose-stimulated insulin secretion by the pancreas [69, 70]. The most intensively studied incretins, glucagon-like peptide-1 (GLP-1) and glucose-dependent insulinotropic polypeptide (GIP), are now known to play important roles in the brain [69, 71-73], including in regions that show pathological features of AD and/or PD (i.e., cerebral cortex, hippocampal formation, striatum, and substantia nigra/ventral tegmental area), where GLP-1 receptors (GLP-1Rs) [74-79] and/or GIP receptors (GIPRs) [80-83] are expressed. At present, there are two types of IRAs: those that activate receptors for one type of incretin (single IRAs) and those that activate receptors for both types of incretins (dual IRAs). The single IRAs thus far demonstrating the greatest promise as AD and/or PD therapeutics are the FDA approved GLP-1 receptor agonists (GLP-1RAs) exendin-4 (Byetta®) [42, 43, 56-58, 65-67, 84], liraglutide (Victoza®) [36-41, 43, 48-50, 53, 85], lixisenatide (Adlyxin® in the U.S., Lyxumia® in Europe) [40, 45, 53], and semaglutide (Ozempic®) [61, 62]. The dual IRAs showing promise as therapeutics for those disorders do not have generic names yet. We refer to them simply as Peptide 18 (from B. Finan and T. Ma, co-first authors of the paper reporting synthesis of this peptide [86]) and DA-JC4 [44, 59]. DA3-CH [60], and DA5-CH [46, 47, 59, 63] (from C. Hölscher, director of the lab introducing these peptides). Of these, Peptide 18, DA-JC4, and DA5-CH are of special interest since their therapeutic potency is greater than that of single IRAs [59, 60, 63].

1.3. The importance of pharmacokinetic studies in assessing relative IRA brain uptake

To determine which IRAs are the best candidate AD and PD therapeutics, we need to know their relative ability to completely cross the blood-brain barrier (BBB) and enter the central nervous system (CNS). While a pharmacokinetic study by Kastin and Akerstrom [87] showed that exendin-4 does cross the BBB in mice, no such study has been published on other IRAs.

The need for rigorous pharmacokinetic studies on other IRAs is illustrated by conflicting reports on brain uptake of liraglutide. Studies that have suggested liraglutide crosses the BBB, have not taken into consideration brain capillary binding or sequestration [46, 63, 88].

Other studies have suggested liraglutide accumulates within circumventicular organs (CVOs) [89-91], small brain regions lacking a BBB and regulating metabolic state (i.e., the median eminence) [99].

1.4. Objectives of this study

To resolve the noted inconsistencies in the literature on brain influx of liraglutide and to extend them to virtually all IRAs showing promise as AD and PD therapeutics, the present study compared the pharmacokinetics of ^{125}I-labeled single IRAs (exendin-4, liraglutide, lixisenatide, and semaglutide) and ^{125}I-labeled dual IRAs (Peptides 17, 18, and 20, as well as DA3-CH and DA-JC4) injected intravenously (iv) in adult mice. DA5-CH was not tested, because it proved refractory to successful iodination. Given the number of IRAs tested, this initial study focused on whole brain analyses.

For each peptide tested, we determined the rate of clearance from serum, the rate of unidirectional brain influx, degree of transport across capillaries into brain parenchyma, percentage of the dose taken up per gram of brain tissue, degradation rate of iodinated peptides in serum and brain, and saturability of the influx rate. Additional tests were run to determine the mechanism of exendin-4 brain influx and whether liraglutide brain-to-blood (efflux) occurs. Of the nine IRAs tested, exendin-4 and the dual IRA derivative DA-JC4 showed the fastest rates of brain influx and significant accumulation in brain parenchyma.

2. Materials and methods

2.1. Peptide sources

Exendin-4, liraglutide, and Peptides 17, 18, and 20 were supplied by Dr. Richard D. DiMarchi at Indiana University. The sequence and synthesis of these peptides are described in Finan and Ma *et al.* [86]. Derivatives of Peptide 17 (DA-CH3, DA-J4, and DA5-CH) were synthesized by ChinaPeptide Co., Ltd. (Shanghai, China) for Dr. Christian Hölscher, who supplied them for this study. Lixisenatide and semaglutide were purchased from BOC Sciences (Shirley, NY), catalog numbers B0084-090106 and B0084-007194, respectively. Sequences and additional peptide information are listed in Table 1.

2.2. Animal use

Male CD-1 mice (8-10 weeks old) purchased from Charles River Laboratories (Wilmington, MA) were used for all studies. They had *ad libitum* access to food and water and were kept on a 12 h light/12 h dark cycle. All animal studies were approved by the Institutional Animal Care and Use Committee (IACUC) at the Veterans Affairs Puget Sound Health Care System in Seattle, WA in a facility approved by the Association for Assessment and Accreditation of Laboratory Animal Care International (AAALAC). In all studies, mice were first anesthetized with 0.15 mL of 40% urethane via an intraperitoneal (ip) injection.

2.3. Radioactive labeling

The IRAs were radioactively labelled following the protocol outlined in Rhea *et al.* [92]. Ten micrograms of each IRA were labeled with 0.5 mCi Na ^{125}I (Perkin Elmer, Waltham, MA) by reacting it with 10 μg of chloramine-T (Sigma-Aldrich, St. Louis, MO) in 0.25 M

chloride-free sodium phosphate buffer, pH 7.5. After 1 min, the reaction was terminated by adding 100 μg of sodium metabisulfite (Sigma-Aldrich). Bovine serum albumin (BSA, Sigma-Aldrich) was labeled with ^{99m}Technetium (^{99m}Tc, GE Healthcare, Seattle, WA) by combining 1 mCi ^{99m}Tc with 1 mg albumin, 120 μg stannous tartrate, and 20 μL 1M HCl in 500 μL deionized waterfor 20 min. Radioactively labeled IRAs (^{125}I-IRAs) and albumin (^{99m}Tc-Alb) were purified on Sephadex G-10 columns (Sigma-Aldrich), collected in 1% BSA lactated Ringers solution (BSA/LR) and characterized by 15% trichloroacetic acid (TCA, Fisher Scientific) protein precipitation (1 μL radiolabeled peptide, 500 μL BSA/LR, and 500 μL 30% TCA). Greater than 90% radioactivity in the precipitated fraction was consistently observed for the IRAs tested and albumin.

2.4. Octanol/buffer partition coefficient

To measure lipid solubility of the IRAs, 1×10^5 counts per minute (cpm) of an ^{125}I-IRA was added to duplicate tubes containing equal volumes 0.25 M chloride-free sodium phosphate buffer, pH 7.5 and octanol (Sigma-Aldrich). This solution was vigorously mixed and centrifuged to separate the two phases. Aliquots of 100 μL were taken in triplicate from each phase, and total radioactivity was counted in a gamma counter. The measure of lipophilicity equates to the mean partition coefficient expressed as the ratio of the cpm in the octanol phase to the cpm in the buffer phase. The log value for the coefficient can be either greater than unity, indicative of a lipophilic compound, or less than unity, indicative a hydrophilic compound.

2.5. In vivo stability of ^{125}I-IRAs in brain and blood

Following anesthetization, arterial blood and whole brain were taken 10 or 60 min after iv injection of $1x10^6$ cpm of ^{125}I-IRA in 0.2 mL of BSA/LR. The blood samples were allowed to clot, centrifuged at 5400g for 10 min, and 50 μL of the separated serum was added to 250 μL of BSA-LR, mixed and combined with 300 μL of 30% TCA, mixed again, and then centrifuged for 10 min at 5400g. Brains were homogenized in 500 μL of BSA-LR with a bead beater for 30 sec on ice at 4800 rpm twice. Homogenates were centrifuged at 5400g for 15 min, and a portion of the resulting supernatant was added to an equal volume of 30% TCA, mixed, and then centrifuged at 5400g for 10 min. The radioactivity in the resulting S and P fractions for serum and brain was calculated separately, and the percent of radioactivity in the precipitate was calculated as outlined by Rhea *et al.* [92] using the following equation:

$$\%\ \text{Precip} = 100 \times (\text{P}) \ / \ (\text{S+P}) \quad (1)$$

To correct for degradation that might have occurred during the processing, ^{125}I-IRA was added to non-radioactive arterial whole blood or to whole brain and processed as above. The biological samples were corrected for degradation during processing by dividing their values by those for processing control values and multiplying by 100. Processing control values are listed in Table 2.

2.6. Clearance of ^{125}I-IRAs from serum

Following anesthetization, the jugular vein and right carotid artery were exposed. Mice were given an injection into the jugular vein of 0.2 mL BSA-LR containing 1x10^6 cpm of an ^{125}I-labeled IRA and 5x10^5 cpm of ^{99m}Tc-Alb. Blood samples were collected 1 to 60 min after iv injection. Immediately after blood collection, the mouse was decapitated, and the brain was removed and weighed. The arterial blood was centrifuged at 5400g for 10 min at 4°C, and the serum was collected. Levels of radioactivity in serum (50 μL) and brain were measured in a gamma counter (Wizard2, Perkin-Elmer) for 3 min. To determine the rate of ^{125}I-IRA clearance from the serum, the results were expressed as the percentage of an injected dose in each mL of serum (%Inj/mL), which was calculated by dividing the cpm in a mL of serum (cpm/mL serum) by the cpm injected into the mouse (Inj cpm):

$$\%\ \text{Inj/mL} = 100 \times (\text{cpm/mL serum}) \ / \ (\text{mean Inj cpm}) \quad (2)$$

The log(%Inj/mL) was plotted against time to calculate the rate of clearance from the serum. Because we plotted log (%Inj/mL) vs time, the inverse slope (K_i) of the curve for each IRA was multiplied by 0.301 ($\log_{10}(2)$ to determine the half-time clearance in minutes. The blood and brain cpm data were used for the measurement of brain influx and initial volume of distribution in brain as described in Section 2.7.

2.7. Measurement of brain influx and initial volume of distribution in brain

To calculate the blood-to-brain unidirectional influx rate (K_i) multiple-time regression analysis was used as detailed previously [92-94]. The brain/serum (B/S) ratios (μL/g) of the ^{125}I-IRA in each gram of brain were calculated from the data in Section 2.6 and plotted against their respective exposure times as previously described by Rhea *et al.* [92]. B/S ratios were corrected for vascular space by subtracting the B/S ratio for ^{99m}Tc-Alb (delta B/S ratio). Exposure time differs from clock time in that exposure time corrects for ^{125}I-IRA serum clearance and thus, better represents the amount of ^{125}I-IRA available for BBB transport at any given time. The slope of the linear portion of the relationship between B/S ratios and exposure time defines K_i (μL/g-min) and is reported with its error term. The y-intercept of this linear portion of the relationship defines V_i, (μL/g), the initial volume of distribution in brain at t = 0, which is the functional volume per unit brain mass of a soluble compound that exchanges rapidly and reversibly with plasma [94].

2.8. Percent of injected dose taken up by the brain

For IRAs that showed transport into the brain, the percentage of the iv injected dose taken up by each gram of brain tissue (%Inj/g) was calculated using the following equation:

$$\%\ \text{Inj/g} = (\text{Am/Cpt} - V_i) \times (\%\ \text{Inj/mL}) \quad (3)$$

where Am is cpm/g of brain, Cpt is cpm/mL arterial serum at time t, and V_i corrects the B/S ratio for the amount of peptide reversibly binding the endothelium.

2.9. Saturability of brain uptake

To determine whether brain uptake of each IRA was saturable, some anesthetized mice were co-injected iv with 1 μg of the non-radioactive IRA with $1x10^6$ cpm ^{125}I-IRA and $5x10^5$ cpm of ^{99m}Tc-Alb in 0.2 mL BSA-LR. Blood was collected from the right carotid artery, and the whole brain was removed and weighed at 15 min after iv injection. Results were expressed as B/S ratios in units of μL/g.

2.10. Capillary depletion without vascular washout

The capillary depletion method was used to separate cerebral capillaries and vascular components from brain parenchyma following the methods described by Rhea *et al.* [92]. Anesthetized mice received an iv injection of $1x10^6$ cpm of an ^{125}I-IRA with $5x10^5$ cpm ^{99m}Tc-Alb BSA-LR and 15 min later, blood and brains were collected. Whole brains were homogenized in glass with physiological buffer (10 mM HEPES, 141 mM NaCl, 4 mM KCl, 2.8 mM $CaCl_2$, 1 mM $MgSO_4$, 1 mM NaH_2PO_4, and 10 mM D-glucose adjusted to pH 7.4), mixed with 26% dextran (Sigma-Aldrich), and centrifuged at 5400g for 15 min at 4°C. The pellet, which contained the capillaries, and the supernatant, which contained the brain parenchymal/interstitial fluid space, were carefully separated. The ratio of ^{125}I-IRA radioactivity in the supernatant (parenchyma) was corrected for vascular space by subtracting the B/S ratio of ^{99m}Tc-Alb in the supernatant. The parenchyma/serum and capillary/serum ratios (μL/g) were calculated as (cpm/g tissue)/(cpm/μL) serum.

2.11. Measurement of exendin-4 uptake by adsorptive transcytosis

Following anesthetization, the jugular vein and right carotid artery were exposed. They were then given a jugular vein injection of 0.2 mL BSA-LR containing $1x10^6$ cpm of ^{125}I-exendin-4 and $5x10^5$ cpm of ^{99m}Tc-Alb. In some mice, 10 μg/mouse of a plant lectin (wheat germ agglutinin [WGA], Sigma-Aldrich) was included in the iv injection [95, 96]. Brain and serum samples were collected between 1 and 10 minutes. At each time point, the B/S ratio of ^{125}I-exendin-4 was calculated as in section 2.7 and corrected for vascular space using ^{99m}Tc-Alb B/S ratios. Brain influx rates (K_i) with and without WGA over the course of the course of the experiment were expressed in μL/g-min.

2.12. Liraglutide efflux transport from brain to blood

An intracerebroventricular (ICV) method [97, 98] was used to assess brain-to-blood efflux rate of liraglutide. In anesthetized mice, the scalp was removed, a hole was made in the skull (0.5mm posterior and 1 mm lateral to bregma), and a 26-gauge needle with a tubing guard was used to keep the depth of the hole constant (3.0-3.5 mm). One μL of LR containing 2.5×10^4 cpm of ^{125}I-liraglutide was injected ICV into the lateral ventricle using a 1.0 μL Hamilton syringe. For self-inhibition studies, 1 μg of unlabeled liraglutide was co-injected with 2.5×10^4 cpm of ^{125}I-liraglutide ICV. Whole brain was removed and weighed 10 min later. The level of ^{125}I-liraglutide available for transport at t = 0 was estimated by repeating the procedure in mice that had been overdosed with urethane and had been dead for 10-20 min [97, 98]. Levels of radioactivity in the brain samples were counted for 3 minutes in a gamma counter and divided by the amount injected and the brain weight in grams to yield the percentage of ^{125}I-liraglutide injected remaining per gram brain weight (%Inj/g). The

amount of ^{125}I-liraglutide that was available for transport out of the brain (%T) was determined with the equation:

$$\%T = 100 \times [(\%Inj/g)_0 - (\%Inj/g)_{10}] \; / \; (\%Inj/g)_0 \quad (4)$$

where $(\%Inj/g)_0$ is the mean level of %Inj/g for the t = 0 group and $(\%Inj/g)_{10}$ is the individual mouse's level of %Inj/g at t = 10 min.

2.13. Statistical analyses

Regression analysis and other statistical analyses were performed with the use of Prism 8.0 (GraphPad Software Inc., San Diego, CA). Means are reported with their standard error and compared by one-way analysis of variance (ANOVA) followed by the Newman-Keuls post-hoc test. Linear and non-linear regression lines are reported with their correlation coefficients and n values. Multiple-time regression analyses were used to compare changes in variables over time. T-tests were used to analyze results when only two experimental groups were compared. Statistical significance was defined as $p < 0.05$.

3. Results

3.1. Properties of the IRAs studied

Table 1 provides basic information on the 9 IRAs studied, all of which are 31-45 amino acid (aa) peptides. The GLP-1R mimetic exendin-4, the GLP-1R analogue lixisenatide, and the dual GLP-1R/GIPR agonist Peptide 17 are unbranched peptides, the last of which is referred to here as the native or unmodified dual IRA. The GLP-1 analogues liraglutide and semaglutide are acylated. The other 4 tested IRAs are modified versions of Peptide 17 with Peptide 18 being an acylated version, Peptide 20 being a PEGylated version, and DA3-CH and DA-JC4 being versions with modified C-termini in which the final cysteine is replaced by a lysine in DA3-CH or 6 lysines in DA-JC4. All the peptides except lixisenatide and DA-JC4 are negatively charged, especially exendin-4 and Peptide 17, with roughly equivalent percentages of hydrophobic residues (32-41%). Lixisenatide and DA-JC4 are positively charged and contain equivalent percentages of hydrophobic residues (44-50%). We found that the acylated dual agonist (Peptide 18) is significantly more lipid soluble than all the other tested IRAs (partition coefficient = 0.249 ± 0.02), including the other acylated peptides, namely liraglutide (partition coefficient = 0.0123 ± 0.00) and semaglutide (partition coefficient = 0.0353 ± 0.00).

3.2. Degradation in serum and whole brain

To confirm that radioactivity measured in serum and whole brain tissue was intact ^{125}I-IRAs and not free iodine, serum and brain homogenates were acid precipitated. The majority of labeled peptide in the serum remained intact for the duration of the uptake study. Table 2 shows the amount of peptide bound to ^{125}I precipitated with acid at 10 and 60 min. DA3-CH showed the greatest amount of degradation, losing 19.6% in serum from 10 to 60 min and 44.9% over the same period in whole brain. Liraglutide and semaglutide were the most stable, precipitating less than 2% in serum over time and less than 12% in whole brain.

3.3. Clearance from Serum

Fig. 1A shows the clearance of ^{125}I-IRAs from serum after injection. The relation between log levels of the radioactivity in arterial serum expressed as percentage of injected IRA per ml (%Inj/mL) over time during the linear period after iv injection is shown in Fig. 1B. Linear regression analysis showed a statistically significant relation between log (%Inj/mL) and time for all peptides. ^{125}I-Peptide 18 had the fastest clearance (32.37 min) while ^{125}I-liraglutide had the slowest clearance (167.22 min). The half-time clearance rates for all the peptides tested are listed in Table 3.

3.4. Whole brain influx and initial volume of distribution

The brain influx rate of all 9 ^{125}I-IRAs calculated from the B/S ratios is graphed in Fig. 2. The full curve is presented in Fig. 2A, while the linear rate of transport is shown in Fig. 2B. A blood-to-brain unidirectional influx rate (K*i*) was measurable for all the ^{125}I-IRAs except for ^{125}I-liraglutide, ^{125}I-semaglutide, and ^{125}I-Peptide 18, in which there was no significant relationship between B/S ratios and exposure time.

The unidirectional blood-to-brain influx rate K*i* for the 9 IRAs tested is graphed in Fig.3. Table 3 lists the K_i and V_i values for each IRA. As seen in that table, significant K*i*'s were found only for non-acylated and non-PEGylated IRAs. Among those IRAs, the rank order of brain influx rates were as follows from highest to lowest: (1) ^{125}I-DA-JC4 (K*i* = 0.6680 ± 0.1089 μL/g - min, r = 0.8707, p < 0.0001), (2) ^{125}I-exendin-4 (K*i* = 0.423 ± 0.0703 μL/g - min, r = 0.8191, p = 0.0003), (3) ^{125}I-DA3-CH (K*i* = 0.3922 ± 0.0668 μL/g - min, r = 0.7418, p < 0.0001), (4) ^{125}I-Peptide 17 (K*i* = 0.3489 ± 0.0228 μL/g - min, r = 0.0151, p< 0.0001), (5) ^{125}I-lixisenatide (K*i* = 0.3271 ± 0.0726 μL/g - min, r = 0.6924, p = 0.0015), and (6) ^{125}I-Peptide 20 (K*i* = 0.0890 ± 0.0382 μL/g - min, r = 0.5750, p = 0.0398). The brain influx rate thus differed over 50-fold among the IRAs tested. The initial volume of distribution V_i in brain at t = 0 min was highest for ^{125}I-DA-JC4 at 2.495 ± 0.8554 μL/g, while that for ^{125}I-Peptide 20 was the lowest at 0.4075 μL/g ± 0.2728, suggesting DA-JC4 has a greater level of binding at the brain vascular endothelium compared to Peptide 20; V_i's for the other IRAs are listed in Table 3. No ^{99m}Tc-Alb uptake was observed during this period as expected (data not shown). The K_i did not correlate with the solubility octanol partition coefficient, the octanol partition coefficient divided by the square root of the molecular weight, nor the log of the octanol partition coefficient divided by the square root of the molecular weight (data not shown).

The percent of injected ^{125}I-IRAs taken up per gram brain tissue (%Inj/g) is shown in Fig. 4, except for the ^{125}I-IRAs that did not exhibit significant BBB transport: liraglutide, semaglutide, and Peptide 18. The data are based on the influx rate depicted in Fig. 2. By 60 min, the percent was highest by far for ^{125}I-exendin-4 (0.54%) and was continuing to rise. For all the other ^{125}I-IRAs with significant K*i*s, the percent plateaued by 30 min. For these, the peak %Inj/g percent was highest for ^{125}I-DA-JC4 (0.17%), somewhat lower for ^{125}I-Peptide 17 (0.15%), and much lower for ^{125}I-DA3-CH (0.08%), ^{125}I-Peptide 20 (0.05%) and ^{125}I-lixisenatide (0.05%).

3.5. Saturability of transport across the BBB

To help characterize the nature of IRA whole brain uptake after iv injection and determine if transport occurred in a saturable manner, we injected each ^{125}I-IRA with or without its non-radioactive form. Inclusion of the non-radioactive IRA (1 μg/mouse) with the ^{125}I-IRA 15 min after injection did not affect the B/S ratios of all ^{125}I-IRAs, except ^{125}I-liraglutide. Co-injection of non-radioactive liraglutide (1 μg/mouse) with ^{125}I-liraglutde *increased* its B/S ratio (8.02 ± 1.554 μL/g for ^{125}I-liraglutide alone vs. 9.86 ± 1.784 μL/g for ^{125}I-liraglutide + the unlabeled drug, $p < 0.05$, n = 8 mice/group, Table 4). Serum cpm/μL was *decreased* when ^{125}I-liraglutide was co-injected with unlabeled liraglutide (573.1 ± 59.48 cpm/μL vs. 447.8 ± 38.17 cpm/μL, $p < 0.001$), which was also seen when ^{125}I-Peptide 18 was co-injected with unlabeled Peptide 18 (422.7 ± 74.96 cpm/μL vs. 349.4 ± 57.98 cpm/μL, $p < 0.05$).

3.6. Uptake by brain parenchyma

To determine if the iodinated IRAs were transported into brain parenchyma rather than being sequestered by vascular endothelial cells, we performed capillary depletion studies. This is necessary to verify transport of a drug across the endothelial cell wall. The percent of each IRA reaching the brain that was found in parenchyma vs capillaries (Table 3) was highest for DA-JC4 (89.72%) followed by DA3-CH (86.02%), exendin-4 (84.2%), lixisenatide (66.8%), and Peptide 17 (73.2%). The majority of Peptide 20 (56.4%) and liraglutide (71.3%) was trapped in the capillaries. Semaglutide and Peptide 18 appeared completely sequestered by the capillaries as none of the ^{125}I-semaglutide or Peptide18 was detected in brain parenchyma.

3.7. Testing adsorptive transcytosis as a mechanism for exendin-4 brain influx

A common mechanism of transfer across the BBB is that of adsorptive transcytosis. We tested this for exendin-4 whose K*i* was the highest found in this study. As shown in Fig. 5, addition of WGA significantly increased the rate of ^{125}I-exendin-4 brain uptake by about 45% ($p = 0.0015$). The rate of transport with the addition of WGA was 0.5683 ± 0.0611 μL/g - min ($r = 0.9371$, $p < 0.001$), while the rate in the absence of WGA was 0.3153 ± 0.0338 μL/g - min ($r = 0.9375$, $p < 0.001$). Enhanced transport occurred without affecting permeability of the BBB to ^{99m}Tc-Alb, demonstrating that WGA did not disrupt the BBB (data not shown).

3.8. Characterization of BBB efflux of liraglutide from the brain

One cause of a paradoxic negative relation between B/S ratios as well as an increase in transport across the BBB with the addition of unlabeled material as seen for liraglutide is the presence of an efflux (i.e., brain-to-blood) transporter. Efflux of ^{125}I-liraglutide was measured by its disappearance from whole brain after an ICV injection. As shown in Fig. 6, ^{125}I-liraglutide efflux was not inhibited by ICV injection of unlabeled liraglutide, demonstrating that its clearance is probably not regulated by a saturable system (52.05% ^{125}I-liraglutide alone vs. 53.96% ^{125}I-liraglutide + unlabeled liraglutide).

4. Discussion

Defining the pharmacokinetics of IRA BBB transport helps to elucidate the direct therapeutic potential of drugs administered systemically for AD [36, 64] or PD [65, 66, 68], including animal models of AD [37-46, 48-50, 99] and PD [51-53, 55-63, 84]. While an intranasal route of administration may be the most efficient means of delivering IRAs to the brain judging from studies on exendin-4 [100]. GLP-1 [101], and the GLP-1R antagonist exendin 9-39 [102], a systemic route for an IRA with CNS access has the advantage of targeting both brain and systemic insulin resistance. This is advantageous because many AD and PD cases with cognitive impairment suffer not only from brain insulin resistance [25, 28, 29], but also from systemic insulin resistance [14-17, 103]. Like T2D, systemic insulin resistance is itself a risk factor for AD [104-107] and possibly PD [18, 103], especially PD with dementia [103].

It is thus important to determine which systemically administered IRAs can cross the BBB and thereby widely target both brain and systemic insulin resistance. We provide here the first pharmacokinetic study comparing the relative ability of IRAs to cross the BBB, specifically 4 single IRAs (i.e., the GLP-1RAs exendin-4, liraglutide, lixisenatide, and semaglutide), 3 dual IRAs of Finan and Ma et al. [86] (i.e., the unbranched GLP-1R/GIPR agonist Peptide 17, its acylated form Peptide 18, and its PEGylated form Peptide 20), and 2 dual IRAs of C. Hölscher derived from Finan and Ma et al.'s [86] Peptide 17 in which the C-terminal cysteine is replaced by a single lysine (DA3-CH) [60] or by 6 lysines (DA-JC4) [59].

4.1. Stability of ^{125}I-IRAs in serum and whole brain

The iodinated IRAs we studied remained primarily intact in serum over 60 min. At least 75% of ^{125}I radioactivity in each iodinated dose was recovered in precipitated serum peptides at 60 min. Brain levels of ^{125}I radioactivity detected in our experiments could thus be attributed primarily to uptake of intact IRAs. At least 75% of ^{125}I radioactivity in each iodinated dose was also recovered in precipitated peptides in brain homogenates at 60 min for liraglutide, lixisenatide, semaglutide, Peptide 18, and Peptide 20. Lesser brain recovery at 60 minutes was obtained, however, for iodinated IRAs with the fastest uptake rates: 48% for DA-JC4 (K_i = 0.668 ± 0.11 μl/g - min), 37.7% for exendin-4 (K_i = 0.423 ± 0.07 μl/g - min), and 26.7% for DA3-CH (K_i = 0.392 ± 0.07 μl/g - min). It should be noted that the K_i's were determined, as required for the multiple-time regression analysis, on only the linear portion of the relation between B/S ratios and Expt. The lowest value for precipitation during the linearity was 69.63% for brain and 85.66% for serum, both for DA-JC4.

The findings suggest that the IRAs with the fastest brain uptake are more rapidly metabolized in brain than in serum. There are several possible explanations for this. First, the radioactive iodine labels a tyrosine and the brain is abundant in iodotyrosinases. Thus, the radioactive iodine can be quickly cleaved from the peptide soon after entering the brain, leaving free iodide which is poorly precipitated by acid. Second, transport by the route of adsorptive transcytosis classically involves routing to the lysosomal compartment resulting in degradation of peptide during its passage across the BBB [108-110]. Lastly, two enzymes classically degrade IRAs: dipeptidyl peptidase-4 (DPP-4) and neprilysin, also known as

neutral endopeptidase or enkephalinase [111, 112]. DPP-4 is not expressed in the rodent brain [113] and neprilysin activity in mouse brain [114] is not higher than it is in mouse plasma, whereas DPP-4 activity is higher in mouse plasma than neprilysin activity [115]. Irrespective of brain degradation, the serum degradation values suggest the peptides were intact at the time of transport.

4.2. Relative brain influx rates of IRAs and their saturability

Brain influx rates (K_i in μL/g-min) were calculated for all ^{125}I-IRAs and are listed in order starting with the fastest transport rate: DA-JC4 (0.6680) > exendin-4 (0.4231) > DA3-CH (0.3922) > Peptide 17 (0.3489) > lixisenatide (0.3271) >> Peptide 20 (0.0892). The calculated exendin-4 K_i matches with previous literature [87]. There was no statistically significant correlation between the B/S ratios and the exposure time for the acylated IRAs liraglutide, semaglutide, or Peptide 18, indicating lack of transport. These data are consistent with brain uptake rates of fluorescently labeled IRAs [46, 63]. This suggests that acylation of IRAs impairs their ability to cross the BBB. While acylation classically increases transmembrane diffusion across the BBB [116], it can also enhance stability of a peptide in serum by increasing albumin binding [117]. This modification can also affect the physical stability leading to the formation of oligomers, as is the case for liraglutide [118], which might impact the ability to cross the BBB.

An explanation for the negative K_i of ^{125}I-liraglutide and for its paradoxic increase in brain uptake when co-injected with unlableled liraglutide is the presence of a brain-to-blood efflux transporter. However, co-injecting unlabeled liraglutide along with ^{125}I-liraglutide into the lateral ventricle of the brain (1 μg) did not alter ^{125}I-liraglutide efflux from the brain. Therefore, a brain *efflux* transporter is likely not a contributor to the lack of liraglutide accumulation by brain observed here. Our results are consistent with studies of GLP-1 pS8 and exendin-4 [87, 119], which showed no evidence of a rapid efflux transport system for these GLP-1-like peptides.

Since the B/S ratio of all ^{125}I-labeled IRAs studied, except liraglutide, was unaffected by addition of a 1 μg iv dose of the unlabeled IRA, these peptides do not appear to cross the BBB by a saturable process. This is consistent with a previous study showing that brain influx of an ^{125}I-labelled, degradation-resistant GLP-1 analog, GLP-1 pS8, is not inhibited by 5 μg of the unlabeled peptide [119], but is inconsistent with a study showing that ^{125}I-exendin-4 brain influx is weakly inhibited by 5 μg of unlabeled exendin-4 [87]. However, if transport is saturable, the 1 μg iv competition dose should be sufficient to affect transport at a therapeutic level as it is 1000 fold greater than a common dose given in clinical studies (2 mg sc) [120]. Even if transport is saturable at greater doses, saturability likely occurs at therapeutically irrelevant levels.

4.3. Relative total influx of IRAs into brain and its parenchyma

To quantify how much of each IRA injected can enter the brain, we calculated the percentage of the injected dose per gram of brain tissue (%Inj/g). It should be noted the amounts of each drug we injected were sub-micromolar as radioactivity allows us to work with extremely low levels of peptide, providing a much greater signal to noise ratio in

detecting BBB transport rates without affecting physiology. On this parameter, the percentages ranged over 20-fold, from 0.025-0.56 %Inj/g. Exendin-4 was exceptional in this regard at 0.56 %Inj/g and still rising at the final 60 min time point, suggesting that an even greater amount of this GLP-1 analog would be present in brain at later time points. As expected based on its K_i, DA-JC4 had the next highest percentage of injected drug entering the brain (0.17 %Inj/g). This percentage is in the range of hormones crossing the BBB that affect insulin-related functions, including insulin (0.046%) [121], amylin (0.12%) [121], ghrelin (0.063%) [122], and leptin (0.171%) [123].

Rarely, substances taken up by brain endothelial cells are sequestered by them rather than completing the transport into the brain parenchymal space. Small amounts of peptide are expected in capillaries as transit is a time-dependent process, but large amounts in capillaries may indicate a block to complete passage across the capillary wall. Our capillary depletion studies indicated that the ^{125}I-IRAs tested varied in their ability to completely cross the capillary wall and enter brain parenchyma. Within 15 minutes of iv injection, the majority of DA-JC4, DA3-CH, exendin-4, Peptide 17, and lixisenatide reaching the brain entered its parenchyma. On the other hand, within this same time interval, the majority of Peptide 20 and of liraglutide was sequestered in brain endothelial cells. Semaglutide and Peptide 18 could not be reliably detected in brain parenchyma.

Of the 9 IRAs studied, then, the single IRA exendin-4 and the dual IRA DA-JC4 are best able to cross the BBB based on their rate of brain influx (K*i*), percentage reaching the brain that was found in parenchyma versus capillaries (% parenchyma), and percentage of systemic dose taken up per gram of brain tissue (%Inj/g). With the possible exception of DA5-CH, which we were unable to test as explained earlier, our findings thus identify exendin-4 and DA-JC4 as the IRAs best able to reach the whole brain, including both forebrain and brainstem, structures pathological in AD and/or PD. Future studies should be designed to investigate the regional transport of the IRAs as BBB transport kinetics can vary regionally [87, 124]. Exendin-4 and DA-JC4 consequently merit primary interest among the tested IRAs as therapeutics for these disorders, in which brain insulin resistance is likely to play an important role [16, 25, 28-31, 125]. DA-JC4 deserves special attention in this regard, because a similar dual IRA (Peptide 18) is more potent than a single IRA (liraglutide) or a GIPR agonist (D-Ala^2-GIP) in reducing insulin resistance in the hippocampal formation from AD cases when administered directly to such tissue [35].

4.4. Probable adsorptive transcytosis of non-acylated and non-PEGylated IRAs

As noted in section 4.2, the IRAs best able to cross the BBB were non-acylated and non-PEGylated, specifically the single IRAs exedin-4 and lixisenatide and the dual IRAs Peptide 17, DA3-CH, and DA-JC4. We found no correlation between transport rate and lipid solubility/molecular weight, making transcellular diffusion an unlikely mechanism for this class of peptides. The inability to demonstrate self-inhibition with reasonable doses of unlabeled peptide make saturable mechanisms like carrier transporters and receptor-mediated transport unlikely. The lack of saturable transport mechanism is consistent with studies so far showing no established GLP-1 or GIP receptors on endothelial cells in the adult CNS [74-82, 90, 126, 127]. Indeed, immunoEM of the arcuate hypothalamus in adult

rats [90] revealed no endothelial GLP-1Rs despite clear detection of GLP-1Rs in tanycytes there. Usdin et al. [80] do mention finding GIPR in endothelia of large blood vessels in the rat brain, but they do not show that in their figures nor state if that was seen in their embryonic and/or adult tissue samples.

Adsorptive transcytosis, by contrast, appears the most likely means by which non-acylated and non-PEGylated IRAs cross the BBB. This is a process in which blood-borne substances adhere non-specifically to the luminal surface of endothelial cells, are endocytosed at that surface into vesicles that are transported directly or indirectly to the abluminal surface, where they are exocytosed into interstitial fluid of brain parenchyma [108, 109]. Such a process is consistent with the relative unsaturability of brain influx shown by the non-acylated and non-PEGylated IRAs (see section 4.2) and the net positive charge of lixisenatide and DA-JC4 (see Table 1).

Positive charge has long been considered critical for adsorptive endocytosis and transcytosis given the net negative charge of the luminal and abluminal surfaces of endothelial cells and of the facing basement membrane [108]. Yet recent studies show that negatively charged substances, including small peptides, can cross the BBB by transcytosis [128, 129]. This suggests that negatively charged, non-acylated, non-PEGylated IRAs such as exendn-4, Peptide 17, and DA3-CH may also cross the BBB via adsorptive transcytosis similar to the way WGA crosses that barrier [96]. We tested that with respect to exendin-4 and found that its rate of brain influx was enhanced nearly 45% by co-administration of WGA, a lectin shown to cross by adsorptive transcytosis in brain endothelial cells [130]. Exendin-4 presumably binds to endothelial glycoproteins bound by WGA and is accordingly taken up by WGA-dependent mechanisms. Since WGA did not affect transport of albumin across the BBB (data not shown), it did not enhance exendin-4 influx by disrupting the BBB. Adsorptive transcytosis may thus be the means by which systemically and intranasally administered exendin-4 has been found to reach the cerebral cortex [87, 100].

4.5. Limited brain uptake of liraglutide and semaglutide occurs independent of the BBB

Since systemically administered liraglutide [37-41, 43, 48-50, 53] and semaglutide [61, 62] ameliorate many forebrain and midbrain pathologies in mouse models of AD and/or PD, it was puzzling to find that neither had a significant K*i*. This is not attributable to our use of acute rather than chronic drug administration given a study [90] described earlier (section 1.3). There are several other mechanisms by which circulating substances can influence brain function without crossing the BBB. First, a substance can affect the blood levels of another substance that does cross (i.e., insulin inducing hypoglycemia). Second, a substance can bind to brain endothelial cells without crossing, triggering release of an abluminal substance, such as the case for adiponectin [131, 132]. Third, afferent nerve transmission can be affected (i.e., CCK regulates appetite via the vagus nerve). Lastly, circulating substances can act directly at the CVO to elicit quick actions, the most common examples of which include vomiting, thirst, blood pressure, and temperature.

In the case of liraglutide and semaglutide, it is thought these substances affect brain function by accumulating in brain regions outside to the BBB rather than being transported across the BBB, similar to what we have shown here [89, 90]. These studies have found measureable

levels of these to drugs in 1) CVOs, 2) regions in which the BBB structure fluctuates based on metabolic state (i.e., the hypothalamic arcuate nucleus, and 3) GLP-1R expressing regions near the CVOs or arcuate nucleus, connected by interstitial fluid. However, it is currently unclear how accumulation in these brain regions would affect cognition.

4.6. Rodent versus human BBB

One important consideration to address is the difference between the human and the murine or rodent BBB. Given the BBB structure and function is an understudied field relative to other endothelial beds (i.e., lung or muscle endothelium), we often do not know how much the murine BBB relates to the human. This is compounded by quite different methods used to study the rodent (radioactivity, microdialysis, brain sampling) and human BBB (imaging, CSF sampling). Despite this, there are great similarities between the species in that both transport glucose, have CVOs present, have brain-to-blood efflux systems, and display saturable systems for insulin, leptin, and other substances.

4.7. Relevance to other neurological disorders via multiple therapeutic effects

Our findings are relevant beyond AD and PD, because systemically administered IRAs also show promise in treating other neurological conditions, most notably amyotrophic lateral sclerosis (ALS) [133, 134], stroke [100, 135-140], and traumatic brain injury (TBI) [141].

The promise of IRAs in treating diverse neurological disorders has become increasingly evident with the discovery that such drugs, in addition to more rapidly degraded GLP-1 and GIP, alleviate molecular pathology by diverse mechanisms. Apart from reducing brain insulin resistance, these therapeutic effects fall into the following 5, not necessarily mutually exclusive, categories.

a. Reducing atherosclerosis [142, 143]

b. Diminishing BBB dysfunction [37, 138, 144, 145]

c. Enhancing neurogenesis in the dentate gyrus [38-41, 81, 88, 146-150]

d. Promoting neuroprotection in many, not necessarily mutually exclusive, ways, specifically by enhancing DNA repair [151]; increasing expression and signaling of brain-derived neurotrophic factor (BDNF) [55, 152, 153]; reducing Aβ oligomers [38], Aβ plaque load [38-40, 154-157], Aβ toxicity [158-162], advanced glycation end products [163], apoptosis [44, 100, 135, 136, 164-167], excitotoxicity [168-171], neuroinflammation [38-41, 44, 60, 135, 155-157, 172], endoplasmic reticulum stress [43], oxidative stress [155, 173], tau hyperphosphorylation [44, 46, 48, 163]; pathological reduction of dopamine in the substantia nigra/ventral tegmental area and striatum [51-53, 55-63, 84]; and synaptic degeneration [38-41, 154, 156, 157], and

e. Facilitating synaptic plasticity and cognitive function [38-41, 50, 147, 148, 154, 156-160, 162, 174-183].

4.8. Conclusions

- Within 10 min of iv administration, non-acylated and non-PEGylated IRAs (i.e., exendin-4, lixisenatide, Peptide 17, DA3-CH and DA-JC4) display significant rates of blood-to-brain influx (K*i*'s), whereas acylated IRAs (i.e., liraglutide, semaglutide, and Peptide 18) do not.
- Our results indicated that the acylated IRAs liraglutide and semaglutide do not cross the BBB when assessed for whole brain. Future studies are needed, however, to determine if there is regional transport to key brain areas known to accumulate immunoactive levels of liraglutide following systemic administration and known to have therapeutic effects in AD and PD animal models.
- The non-acylated IRAs are nevertheless of greater interest in treating AD and PD when systemiclly administered because they have the ability to access directly and broadly pathologic brain areas. Brain Influx of non-acylated (and non-PEGylated) IRAs is not a saturable process up to 1 μg of these drugs and is most likely mediated by adsorptive transcytosis across brain endothelial cells, consistent with our WGA test of exendin-4.
- Of the 9 tested peptides, the single IRA exendin-4 and the dual IRA DA-JC4 were best able to cross the BBB based on their rate of brain influx, percentage reaching the brain that accumulate in brain parenchyma, and percentage of the systemic dose taken up per gram of brain tissue. Exendin-4 and DA-JC4 thus deserve priority among the IRAs tested as potential AD and PD therapeutics.
- Finally, our results on IRAs with a wide rage of structural variation should aid in design of new IRAs to achieve greater rates of brain uptake across the BBB and thus greater therapeutic effects on brain pathologies in AD and PD, as well as in ALS, stroke, and TBI, animal models of which are also showing therapeutic benefits from IRA treatment.

Acknowledgements

We would like to thank Dr. Richard D. DiMarchi for supplying us with exendin-4, liraglutide, and 3 dual IRAs, (Peptides 17, 18, and 20) and Dr. Christian Hölscher for supplying us with his modified versions of Peptide 17 (DA3-CH. DA5-CH, and DA-JC4).

References:

[1]. Borlongan CV, Burns J, Tajiri N, Stahl CE, Weinbren NL, Shojo H, Sanberg PR, Emerich DF, Kaneko Y, van Loveren HR, Epidemiological survey-based formulae to approximate incidence and prevalence of neurological disorders in the United States: a meta-analysis, PLoS One 8(10) (2013) e78490. [PubMed: 24205243]

[2]. Erkkinen MG, Kim M-O, Geschwind MD, Clinical Neurology and Epidemiology of the Major Neurodegenerative Diseases, Cold Spring Harb Perspect Biol 10(4) (2018) a033118. [PubMed: 28716886]

[3]. A.s. Association, 2016 Alzheimer's disease facts and figures, Alzheimer's & Dementia 12(4) (2016) 459–509.

[4]. Buckley JS, Salpeter SR, A Risk-Benefit Assessment of Dementia Medications: Systematic Review of the Evidence, Drugs & Aging 32(6) (2015) 453–467. [PubMed: 25941104]

[5]. Cummings JL, Morstorf T, Zhong K, Alzheimer's disease drug-development pipeline: few candidates, frequent failures, Alzheimer's Research & Therapy 6(4) (2014) 37.

[6]. Blanco-Silvente L, Capellà D, Garre-Olmo J, Vilalta-Franch J, Castells X, Predictors of discontinuation, efficacy, and safety of memantine treatment for Alzheimer's disease: meta-analysis and meta-regression of 18 randomized clinical trials involving 5004 patients, BMC Geriatrics 18(1) (2018) 168. [PubMed: 30041625]

[7]. Liu PP, Xie Y, Meng XY, Kang JS, History and progress of hypotheses and clinical trials for Alzheimer's disease, Signal transduction and targeted therapy 4 (2019) 29.

[8]. Huang LK, Chao SP, Hu CJ, Clinical trials of new drugs for Alzheimer disease, Journal of biomedical science 27(1) (2020) 18. [PubMed: 31906949]

[9]. Merola A, Zibetti M, Angrisano S, Rizzi L, Ricchi V, Artusi CA, Lanotte M, Rizzone MG, Lopiano L, Parkinson's disease progression at 30 years: a study of subthalamic deep brain-stimulated patients, Brain : a journal of neurology 134(Pt 7) (2011) 2074–84. [PubMed: 21666262]

[10]. AlDakheel A, Kalia LV, Lang AE, Pathogenesis-targeted, disease-modifying therapies in Parkinson disease, Neurotherapeutics : the journal of the American Society for Experimental NeuroTherapeutics 11(1) (2014) 6–23. [PubMed: 24085420]

[11]. Kalia LV, Lang AE, Parkinson's disease, Lancet 386(9996) (2015) 896–912. [PubMed: 25904081]

[12]. Löhle M, Reichmann H, Clinical neuroprotection in Parkinson's disease — Still waiting for the breakthrough, Journal of the Neurological Sciences 289(1) (2010) 104–114. [PubMed: 19772974]

[13]. Kowal SL, Dall TM, Chakrabarti R, Storm MV, Jain A, The current and projected economic burden of Parkinson's disease in the United States, Movement disorders : official journal of the Movement Disorder Society 28(3) (2013) 311–8. [PubMed: 23436720]

[14]. Kuusisto J, Koivisto K, Mykkänen L, Helkala EL, Vanhanen M, Hänninen T, Kervinen K, Kesäniemi YA, Riekkinen PJ, Laakso M, Association between features of the insulin resistance syndrome and Alzheimer's disease independently of apolipoprotein E4 phenotype: cross sectional population based study, BMJ : British Medical Journal 315(7115) (1997) 1045–1049. [PubMed: 9366728]

[15]. Morris JK, Vidoni ED, Perea RD, Rada R, Johnson DK, Lyons K, Pahwa R, Burns JM, Honea RA, INSULIN RESISTANCE AND GRAY MATTER VOLUME IN NEURODEGENERATIVE DISEASE, Neuroscience 270 (2014) 139–147. [PubMed: 24735819]

[16]. Batista AF, Bodart-Santos V, De Felice FG, Ferreira ST, Neuroprotective Actions of Glucagon-Like Peptide-1 (GLP-1) Analogues in Alzheimer's and Parkinson's Diseases, CNS drugs 33(3) (2019) 209–223. [PubMed: 30511349]

[17]. Macesic M, Lalic NM, Kostic VS, Jotic A, Lalic K, Stefanova E, Milicic T, Lukic L, Gajovic JS, Krako N, Impaired Insulin Sensitivity and Secretion in Patients with Alzheimer's Disease: The Relationship with Other Atherosclerosis Risk Factors, Current vascular pharmacology 15(2) (2017) 158–166. [PubMed: 27599805]

[18]. Hogg E, Athreya K, Basile C, Tan EE, Kaminski J, Tagliati M, High Prevalence of Undiagnosed Insulin Resistance in Non-Diabetic Subjects with Parkinson's Disease, Journal of Parkinson's disease 8(2) (2018) 259–265.

[19]. Mielke JG, Taghibiglou C, Liu L, Zhang Y, Jia Z, Adeli K, Wang YT, A biochemical and functional characterization of diet-induced brain insulin resistance, Journal of Neurochemistry 93(6) (2005) 1568–1578. [PubMed: 15935073]

[20]. Pratchayasakul W, Kerdphoo S, Petsophonsakul P, Pongchaidecha A, Chattipakorn N, Chattipakorn SC, Effects of high-fat diet on insulin receptor function in rat hippocampus and the level of neuronal corticosterone, Life Sciences 88(13) (2011) 619–627. [PubMed: 21315737]

[21]. Calvo-Ochoa E, Hernández-Ortega K, Ferrera P, Morimoto S, Arias C, Short-term high-fat-and-fructose feeding produces insulin signaling alterations accompanied by neurite and synaptic reduction and astroglial activation in the rat hippocampus, Journal of Cerebral Blood Flow & Metabolism 34(6) (2014) 1001–1008. [PubMed: 24667917]

[22]. Kothari V, Luo Y, Tornabene T, O'Neill AM, Greene MW, Geetha T, Babu JR, High fat diet induces brain insulin resistance and cognitive impairment in mice, Biochimica et biophysica acta. Molecular basis of disease 1863(2) (2017) 499–508. [PubMed: 27771511]

[23]. Wakabayashi T, Yamaguchi K, Matsui K, Sano T, Kubota T, Hashimoto T, Mano A, Yamada K, Matsuo Y, Kubota N, Kadowaki T, Iwatsubo T, Differential effects of diet- and genetically-induced brain insulin resistance on amyloid pathology in a mouse model of Alzheimer's disease, Molecular Neurodegeneration 14(1) (2019) 15. [PubMed: 30975165]

[24]. Velazquez R, Tran A, Ishimwe E, Denner L, Dave N, Oddo S, Dineley KT, Central insulin dysregulation and energy dyshomeostasis in two mouse models of Alzheimer's disease, Neurobiol Aging 58 (2017) 1–13. [PubMed: 28688899]

[25]. Talbot K, Wang HY, Kazi H, Han LY, Bakshi KP, Stucky A, Fuino RL, Kawaguchi KR, Samoyedny AJ, Wilson RS, Arvanitakis Z, Schneider JA, Wolf BA, Bennett DA, Trojanowski JQ, Arnold SE, Demonstrated brain insulin resistance in Alzheimer's disease patients is associated with IGF-1 resistance, IRS-1 dysregulation, and cognitive decline, J Clin Invest 122(4) (2012) 1316–38. [PubMed: 22476197]

[26]. Spinelli M, Fusco S, Mainardi M, Scala F, Natale F, Lapenta R, Mattera A, Rinaudo M, Li Puma DD, Ripoli C, Grassi A, D'Ascenzo M, Grassi C, Brain insulin resistance impairs hippocampal synaptic plasticity and memory by increasing GluA1 palmitoylation through FoxO3a, Nature Communications 8(1) (2017) 2009.

[27]. Diehl T, Mullins R, Kapogiannis D, Insulin resistance in Alzheimer's disease, Translational research : the journal of laboratory and clinical medicine 183 (2017) 26–40. [PubMed: 28034760]

[28]. Fiory F, Perruolo G, Cimmino I, Cabaro S, Pignalosa FC, Miele C, Beguinot F, Formisano P, Oriente F, The Relevance of Insulin Action in the Dopaminergic System, Frontiers in neuroscience 13 (2019) 868. [PubMed: 31474827]

[29]. Athauda D, Foltynie T, Insulin resistance and Parkinson's disease: A new target for disease modification?, Progress in neurobiology 145–146 (2016) 98–120.

[30]. Talbot K, Wang H-Y, The nature, significance, and glucagon-like peptide-1 analog treatment of brain insulin resistance in Alzheimer's disease, Alzheimer's & dementia : the journal of the Alzheimer's Association 10(1 0) (2014) S12–S25.

[31]. Hölscher C, Brain insulin resistance: role in neurodegenerative disease and potential for targeting, Expert Opinion on Investigational Drugs 29(4) (2020) 333–348. [PubMed: 32175781]

[32]. Yamazaki S, Satoh H, Watanabe T, Liraglutide Enhances Insulin Sensitivity by Activating AMP-Activated Protein Kinase in Male Wistar Rats, Endocrinology 155(9) (2014) 3288–3301. [PubMed: 24949659]

[33]. Noyan-Ashraf MH, Shikatani EA, Schuiki I, Mukovozov I, Wu J, Li RK, Volchuk A, Robinson LA, Billia F, Drucker DJ, Husain M, A glucagon-like peptide-1 analog reverses the molecular pathology and cardiac dysfunction of a mouse model of obesity, Circulation 127(1) (2013) 74–85. [PubMed: 23186644]

[34]. Gastaldelli A, Brodows RG, D'Alessio D, The effect of chronic twice daily exenatide treatment on β-cell function in new onset type 2 diabetes, Clinical endocrinology 80(4) (2014) 545–53. [PubMed: 23574529]

[35]. Talbot JKK, Stucky A, Shah SM, Lee K-C, Bakshi KP, Chattopadhyay M, Khan A, McClean PL, Hölscher C, Samoyedny AJ, Trojanowski JQ, Wilson R, Bennett DA, DiMarchi RD, Wang H-Y, A dual incretin receptor agonist is especially potent in reducing insulin resistance in brains of mild cognitive impairment (MCI) and Alzheimer's disease (ADd) cases. Abstract 410.01, Society for Neuroscience Annual Meeting 2016.

[36]. Gejl M, Brock B, Egefjord L, Vang K, Rungby J, Gjedde A, Blood-Brain Glucose Transfer in Alzheimer's disease: Effect of GLP-1 Analog Treatment, Scientific Reports 7(1) (2017) 17490. [PubMed: 29235507]

[37]. Kelly P, McClean PL, Ackermann M, Konerding MA, Hölscher C, Mitchell CA, Restoration of Cerebral and Systemic Microvascular Architecture in APP/PS1 Transgenic Mice Following Treatment with Liraglutide™, Microcirculation 22(2) (2014) 133–145.

[38]. McClean P, Parthsarathy V, Faivre E, Hölscher C, The diabetes drug Liraglutide prevents degenerative processes in a mouse model of Alzheimer's disease, J Neurosci 31 (2011).

[39]. McClean PL, Hölscher C, Liraglutide can reverse memory impairment, synaptic loss and reduce plaque load in aged APP/PS1 mice, a model of Alzheimer's disease, Neuropharmacology 76 (2014) 57–67. [PubMed: 23973293]

[40]. McClean PL, Hölscher C, Lixisenatide, a drug developed to treat type 2 diabetes, shows neuroprotective effects in a mouse model of Alzheimer's disease, Neuropharmacology 86 (2014) 241–258. [PubMed: 25107586]

[41]. McClean PL, Jalewa J, Hölscher C, Prophylactic liraglutide treatment prevents amyloid plaque deposition, chronic inflammation and memory impairment in APP/PS1 mice, Behavioural Brain Research 293 (2015) 96–106. [PubMed: 26205827]

[42]. Bomfim TR, Forny-Germano L, Sathler LB, Brito-Moreira J, Houzel J-C, Decker H, Silverman MA, Kazi H, Melo HM, McClean PL, Holscher C, Arnold SE, Talbot K, Klein WL, Munoz DP, Ferreira ST, De Felice FG, An anti-diabetes agent protects the mouse brain from defective insulin signaling caused by Alzheimer's disease–associated Aβ oligomers, The Journal of Clinical Investigation 122(4) (2012) 1339–1353. [PubMed: 22476196]

[43]. Lourenco Mychael V., Clarke Julia R., Frozza Rudimar L., Bomfim Theresa R., Forny-Germano L, Batista André F., Sathler Luciana B., Brito-Moreira J, Amaral Olavo B., Silva Cesar A., Freitas-Correa L, Espírito-Santo S, Campello-Costa P, Houzel J-C, Klein William L., Holscher C, Carvalheira José B., Silva Aristobolo M., Velloso Lício A., Munoz Douglas P., Ferreira Sergio T., De Felice Fernanda G., TNF-α Mediates PKR-Dependent Memory Impairment and Brain IRS-1 Inhibition Induced by Alzheimer's β-Amyloid Oligomers in Mice and Monkeys, Cell Metabolism 18(6) (2013) 831–843. [PubMed: 24315369]

[44]. Shi L, Zhang Z, Li L, Hölscher C, A novel dual GLP-1/GIP receptor agonist alleviates cognitive decline by re-sensitizing insulin signaling in the Alzheimer icv. STZ rat model, Behavioural Brain Research 327 (2017) 65–74. [PubMed: 28342971]

[45]. Cai H-Y, Yang J-T, Wang Z-J, Zhang J, Yang W, Wu M-N, Qi J-S, Lixisenatide reduces amyloid plaques, neurofibrillary tangles and neuroinflammation in an APP/PS1/tau mouse model of Alzheimer's disease, Biochemical and Biophysical Research Communications 495(1) (2018) 1034–1040. [PubMed: 29175324]

[46]. Li C, Liu W, Li X, Zhang Z, Qi H, Liu S, Yan N, Xing Y, Hölscher C, Wang Z, The novel GLP-1/GIP analogue DA5-CH reduces tau phosphorylation and normalizes theta rhythm in the icv. STZ rat model of AD, Brain Behav 10(3) (2020) e01505–e01505. [PubMed: 31960630]

[47]. Cao Y, Hölscher C, Hu M-M, Wang T, Zhao F, Bai Y, Zhang J, Wu M-N, Qi J-S, DA5-CH, a novel GLP-1/GIP dual agonist, effectively ameliorates the cognitive impairments and pathology in the APP/PS1 mouse model of Alzheimer's disease, European Journal of Pharmacology 827 (2018) 215–226. [PubMed: 29551659]

[48]. Batista AF, Forny-Germano L, Clarke JR, Lyra E Silva NM, Brito-Moreira J, Boehnke SE, Winterborn A, Coe BC, Lablans A, Vital JF, Marques SA, Martinez AM, Gralle M, Holscher C, Klein WL, Houzel J-C, Ferreira ST, Munoz DP, De Felice FG, The diabetes drug liraglutide reverses cognitive impairment in mice and attenuates insulin receptor and synaptic pathology in a non-human primate model of Alzheimer's disease, J Pathol 245(1) (2018) 85–100. [PubMed: 29435980]

[49]. Qi L, Ke L, Liu X, Liao L, Ke S, Liu X, Wang Y, Lin X, Zhou Y, Wu L, Chen Z, Liu L, Subcutaneous administration of liraglutide ameliorates learning and memory impairment by modulating tau hyperphosphorylation via the glycogen synthase kinase-3β pathway in an amyloid β protein induced alzheimer disease mouse model, Eur J Pharmacol 783 (2016) 23–32. [PubMed: 27131827]

[50]. Hansen HH, Fabricius K, Barkholt P, Niehoff ML, Morley JE, Jelsing J, Pyke C, Knudsen LB, Farr SA, Vrang N, The GLP-1 Receptor Agonist Liraglutide Improves Memory Function and Increases Hippocampal CA1 Neuronal Numbers in a Senescence-Accelerated Mouse Model of Alzheimer's Disease, Journal of Alzheimer's Disease 46(4) (2015) 877–888.

[51]. Jalewa J, Sharma MK, Gengler S, Hölscher C, A novel GLP-1/GIP dual receptor agonist protects from 6-OHDA lesion in a rat model of Parkinson's disease, Neuropharmacology 117 (2017) 238–248. [PubMed: 28223210]

[52]. Cao L, Li D, Feng P, Li L, Xue G-F, Li G, Hölscher C, A novel dual GLP-1 and GIP incretin receptor agonist is neuroprotective in a mouse model of Parkinson's disease by reducing chronic inflammation in the brain, NeuroReport 27(6) (2016) 384–391. [PubMed: 26918675]

[53]. Liu W, Jalewa J, Sharma M, Li G, Li L, Hölscher C, Neuroprotective effects of lixisenatide and liraglutide in the 1-methyl-4-phenyl-1,2,3,6-tetrahydropyridine mouse model of Parkinson's disease, Neuroscience 303 (2015) 42–50. [PubMed: 26141845]

[54]. Li Y, Duffy K, Ottinger M, Ray B, Bailey J, Holloway H, Tweedie D, Perry T, Mattson M, Kapogiannis D, GLP-1 receptor stimulation reduces amyloid-beta peptide accumulation and cytotoxicity in cellular and animal models of Alzheimer's disease, J Alzheimers Dis 19 (2010).

[55]. Ji C, Xue G-F, Lijun C, Feng P, Li D, Li L, Li G, Hölscher C, A novel dual GLP-1 and GIP receptor agonist is neuroprotective in the MPTP mouse model of Parkinson's disease by increasing expression of BNDF, Brain Research 1634 (2016) 1–11. [PubMed: 26453833]

[56]. Bertilsson G, Patrone C, Zachrisson O, Andersson A, Dannaeus K, Heidrich J, Kortesmaa J, Mercer A, Nielsen E, Rönnholm H, Wikström L, Peptide hormone exendin-4 stimulates subventricular zone neurogenesis in the adult rodent brain and induces recovery in an animal model of Parkinson's disease, J Neurosci Res 86(2) (2008) 326–38. [PubMed: 17803225]

[57]. Harkavyi A, Abuirmeileh A, Lever R, Kingsbury AE, Biggs CS, Whitton PS, Glucagon-like peptide 1 receptor stimulation reverses key deficits in distinct rodent models of Parkinson's disease, Journal of Neuroinflammation 5(1) (2008) 19. [PubMed: 18492290]

[58]. Kim S, Moon M, Park S, Exendin-4 protects dopaminergic neurons by inhibition of microglial activation and matrix metalloproteinase-3 expression in an animal model of Parkinson's disease, The Journal of endocrinology 202(3) (2009) 431–9. [PubMed: 19570816]

[59]. Feng P, Zhang X, Li D, Ji C, Yuan Z, Wang R, Xue G, Li G, Hölscher C, Two novel dual GLP-1/GIP receptor agonists are neuroprotective in the MPTP mouse model of Parkinson's disease, Neuropharmacology 133 (2018) 385–394. [PubMed: 29462693]

[60]. Yuan Z, Li D, Feng P, Xue G, Ji C, Li G, Hölscher C, A novel GLP-1/GIP dual agonist is more effective than liraglutide in reducing inflammation and enhancing GDNF release in the MPTP mouse model of Parkinson's disease, European Journal of Pharmacology 812 (2017) 82–90. [PubMed: 28666800]

[61]. Zhang L, Zhang L, Li L, Hölscher C, Neuroprotective effects of the novel GLP-1 long acting analogue semaglutide in the MPTP Parkinson's disease mouse model, Neuropeptides 71 (2018) 70–80. [PubMed: 30017231]

[62]. Zhang L, Zhang L, Li L, Hölscher C, Semaglutide is Neuroprotective and Reduces α-Synuclein Levels in the Chronic MPTP Mouse Model of Parkinson's Disease, Journal of Parkinson's disease 9(1) (2019) 157–171.

[63]. Zhang L, Zhang L, Li Y, Li L, Melchiorsen JU, Rosenkilde M, Hölscher C, The Novel Dual GLP-1/GIP Receptor Agonist DA-CH5 Is Superior to Single GLP-1 Receptor Agonists in the MPTP Model of Parkinson's Disease, Journal of Parkinson's disease 10(2) (2020) 523–542.

[64]. Gejl M, Gjedde A, Egefjord L, Møller A, Hansen SB, Vang K, Rodell A, Brændgaard H, Gottrup H, Schacht A, Møller N, Brock B, Rungby J, In Alzheimer's Disease, 6-Month Treatment with GLP-1 Analog Prevents Decline of Brain Glucose Metabolism: Randomized, Placebo-Controlled, Double-Blind Clinical Trial, Frontiers in aging neuroscience 8 (2016) 108. [PubMed: 27252647]

[65]. Aviles-Olmos I, Dickson J, Kefalopoulou Z, Djamshidian A, Ell P, Soderlund T, Whitton P, Wyse R, Isaacs T, Lees A, Limousin P, Foltynie T, Exenatide and the treatment of patients with Parkinson's disease, The Journal of Clinical Investigation 123(6) (2013) 2730–2736. [PubMed: 23728174]

[66]. Athauda D, Maclagan K, Skene SS, Bajwa-Joseph M, Letchford D, Chowdhury K, Hibbert S, Budnik N, Zampedri L, Dickson J, Li Y, Aviles-Olmos I, Warner TT, Limousin P, Lees AJ, Greig NH, Tebbs S, Foltynie T, Exenatide once weekly versus placebo in Parkinson's disease: a randomised, double-blind, placebo-controlled trial, Lancet (London, England) 390(10103) (2017) 1664–1675.

[67]. Aviles-Olmos I, Dickson J, Kefalopoulou Z, Djamshidian A, Kahan J, Ell P, Whitton P, Wyse R, Isaacs T, Lees A, Limousin P, Foltynie T, Motor and cognitive advantages persist 12 months after exenatide exposure in Parkinson's disease, Journal of Parkinson's disease 4(3) (2014) 337–44.

[68]. Athauda D, Maclagan K, Budnik N, Zampedri L, Hibbert S, Skene SS, Chowdhury K, Aviles-Olmos I, Limousin P, Foltynie T, What Effects Might Exenatide have on Non-Motor Symptoms in Parkinson's Disease: A Post Hoc Analysis, Journal of Parkinson's disease 8(2) (2018) 247–258.

[69]. Campbell Jonathan E., Drucker Daniel J., Pharmacology, Physiology, and Mechanisms of Incretin Hormone Action, Cell Metabolism 17(6) (2013) 819–837. [PubMed: 23684623]

[70]. Drucker DJ, Habener JF, Holst JJ, Discovery, characterization, and clinical development of the glucagon-like peptides, The Journal of clinical investigation 127(12) (2017) 4217–4227. [PubMed: 29202475]

[71]. Muscogiuri G, DeFronzo RA, Gastaldelli A, Holst JJ, Glucagon-like Peptide-1 and the Central/Peripheral Nervous System: Crosstalk in Diabetes, Trends in endocrinology and metabolism: TEM 28(2) (2017) 88–103. [PubMed: 27871675]

[72]. Müller TD, Finan B, Bloom SR, D'Alessio D, Drucker DJ, Flatt PR, Fritsche A, Gribble F, Grill HJ, Habener JF, Holst JJ, Langhans W, Meier JJ, Nauck MA, Perez-Tilve D, Pocai A, Reimann F, Sandoval DA, Schwartz TW, Seeley RJ, Stemmer K, Tang-Christensen M, Woods SC, DiMarchi RD, Tschöp MH, Glucagon-like peptide 1 (GLP-1), Molecular metabolism 30 (2019) 72–130. [PubMed: 31767182]

[73]. Gault VA, RD Lawrence Lecture 2017 Incretins: the intelligent hormones in diabetes, Diabetic Medicine 35(1) (2018) 33–40. [PubMed: 29044772]

[74]. Merchenthaler I, Lane M, Shughrue P, Distribution of pre-pro-glucagon and glucagon-like peptide-1 receptor messenger RNAs in the rat central nervous system, Journal of Comparative Neurology 403(2) (1998) 261–280.

[75]. Alvarez E, Martínez MD, Roncero I, Chowen JA, García-Cuartero B, Gispert JD, Sanz C, Vázquez P, Maldonado A, De Cáceres J, Desco M, Pozo MA, Blázquez E, The expression of GLP-1 receptor mRNA and protein allows the effect of GLP-1 on glucose metabolism in the human hypothalamus and brainstem, Journal of Neurochemistry 92(4) (2005) 798–806. [PubMed: 15686481]

[76]. Cork SC, Richards JE, Holt MK, Gribble FM, Reimann F, Trapp S, Distribution and characterisation of Glucagon-like peptide-1 receptor expressing cells in the mouse brain, Molecular Metabolism 4(10) (2015) 718–731. [PubMed: 26500843]

[77]. Heppner KM, Kirigiti M, Secher A, Paulsen SJ, Buckingham R, Pyke C, Knudsen LB, Vrang N, Grove KL, Expression and distribution of glucagon-like peptide-1 receptor mRNA, protein and binding in the male nonhuman primate (Macaca mulatta) brain, Endocrinology 156(1) (2015) 255–67. [PubMed: 25380238]

[78]. Farr OM, Sofopoulos M, Tsoukas MA, Dincer F, Thakkar B, Sahin-Efe A, Filippaios A, Bowers J, Srnka A, Gavrieli A, Ko BJ, Liakou C, Kanyuch N, Tseleni-Balafouta S, Mantzoros CS, GLP-1 receptors exist in the parietal cortex, hypothalamus and medulla of human brains and the GLP-1 analogue liraglutide alters brain activity related to highly desirable food cues in individuals with diabetes: a crossover, randomised, placebo-controlled trial, Diabetologia 59(5) (2016) 954–65. [PubMed: 26831302]

[79]. Jensen CB, Pyke C, Rasch MG, Dahl AB, Knudsen LB, Secher A, Characterization of the Glucagonlike Peptide-1 Receptor in Male Mouse Brain Using a Novel Antibody and In Situ Hybridization, Endocrinology 159(2) (2018) 665–675. [PubMed: 29095968]

[80]. Usdin TB, Mezey E, Button DC, Brownstein MJ, Bonner TI, Gastric inhibitory polypeptide receptor, a member of the secretin-vasoactive intestinal peptide receptor family, is widely distributed in peripheral organs and the brain, Endocrinology 133(6) (1993) 2861–2870. [PubMed: 8243312]

[81]. Nyberg J, Anderson MF, Meister B, Alborn A-M, Ström A-K, Brederlau A, Illerskog A-C, Nilsson O, Kieffer TJ, Hietala MA, Ricksten A, Eriksson PS, Glucose-Dependent Insulinotropic Polypeptide Is Expressed in Adult Hippocampus and Induces Progenitor Cell Proliferation, The Journal of Neuroscience 25(7) (2005) 1816–1825. [PubMed: 15716418]

[82]. Figueiredo CP, Antunes VLS, Moreira ELG, de Mello N, Medeiros R, Di Giunta G, Lobão-Soares B, Linhares M, Lin K, Mazzuco TL, Prediger RDS, Walz R, Glucose-dependent insulinotropic peptide receptor expression in the hippocampus and neocortex of mesial temporal

lobe epilepsy patients and rats undergoing pilocarpine induced status epilepticus, Peptides 32(4) (2011) 781–789. [PubMed: 21185343]

[83]. Paratore S, Ciotti MT, Basille M, Vaudry D, Gentile A, Parenti R, Calissano P, Cavallaro S, Gastric inhibitory polypeptide and its receptor are expressed in the central nervous system and support neuronal survival, Central nervous system agents in medicinal chemistry 11(3) (2011) 210–22. [PubMed: 21919873]

[84]. Li Y, Perry T, Kindy MS, Harvey BK, Tweedie D, Holloway HW, Powers K, Shen H, Egan JM, Sambamurti K, Brossi A, Lahiri DK, Mattson MP, Hoffer BJ, Wang Y, Greig NH, GLP-1 receptor stimulation preserves primary cortical and dopaminergic neurons in cellular and rodent models of stroke and Parkinsonism, Proceedings of the National Academy of Sciences of the United States of America 106(4) (2009) 1285–90. [PubMed: 19164583]

[85]. Liu Y, Liu F, Grundke-Iqbal I, Iqbal K, Gong CX, Deficient brain insulin signalling pathway in Alzheimer's disease and diabetes, J Pathol 225(1) (2011) 54–62. [PubMed: 21598254]

[86]. Finan B, Ma T, Ottaway N, Müller TD, Habegger KM, Heppner KM, Kirchner H, Holland J, Hembree J, Raver C, Lockie SH, Smiley DL, Gelfanov V, Yang B, Hofmann S, Bruemmer D, Drucker DJ, Pfluger PT, Perez-Tilve D, Gidda J, Vignati L, Zhang L, Hauptman JB, Lau M, Brecheisen M, Uhles S, Riboulet W, Hainaut E, Sebokova E, Conde-Knape K, Konkar A, DiMarchi RD, Tschöp MH, Unimolecular Dual Incretins Maximize Metabolic Benefits in Rodents, Monkeys, and Humans, Science Translational Medicine 5(209) (2013) 209ra151–209ra151.

[87]. Kastin AJ, Akerstrom V, Entry of exendin-4 into brain is rapid but may be limited at high doses, Int J Obes Relat Metab Disord 27 (2003).

[88]. Hunter K, Hölscher C, Drugs developed to treat diabetes, liraglutide and lixisenatide, cross the blood brain barrier and enhance neurogenesis, BMC Neuroscience 13(1) (2012) 1–6. [PubMed: 22214384]

[89]. Secher A, Jelsing J, Baquero AF, Hecksher-Sørensen J, Cowley MA, Dalbøge LS, Hansen G, Grove KL, Pyke C, Raun K, Schäffer L, Tang-Christensen M, Verma S, Witgen BM, Vrang N, Bjerre Knudsen L, The arcuate nucleus mediates GLP-1 receptor agonist liraglutide-dependent weight loss, The Journal of Clinical Investigation 124(10) (2014) 4473–4488. [PubMed: 25202980]

[90]. Gabery S, Salinas CG, Paulsen SJ, Ahnfelt-Rønne J, Alanentalo T, Baquero AF, Buckley ST, Farkas E, Fekete C, Frederiksen KS, Helms HCC, Jeppesen JF, John LM, Pyke C, Nøhr J, Lu TT, Polex-Wolf J, Prevot V, Raun K, Simonsen L, Sun G, Szilvásy-Szabó A, Willenbrock H, Secher A, Knudsen LB, Semaglutide lowers body weight in rodents via distributed neural pathways, JCI Insight 5(6) (2020).

[91]. Kaur C, Ling EA, The circumventricular organs, Histology and histopathology 32(9) (2017) 879–892. [PubMed: 28177105]

[92]. Rhea EM, Salameh TS, Gray S, Niu J, Banks WA, Tong J, Ghrelin transport across the blood-brain barrier can occur independently of the growth hormone secretagogue receptor, Molecular metabolism 18 (2018) 88–96. [PubMed: 30293893]

[93]. Patlak CS, Blasberg RG, Fenstermacher JD, Graphical evaluation of blood-to-brain transfer constants from multiple-time uptake data, J Cereb Blood Flow Metab 3(1) (1983) 1–7. [PubMed: 6822610]

[94]. Blasberg RG, Fenstermacher JD, Patlak CS, Transport of alpha-aminoisobutyric acid across brain capillary and cellular membranes, J Cereb Blood Flow Metab 3(1) (1983) 8–32. [PubMed: 6822623]

[95]. Broadwell RD, Transcytosis of macromolecules through the blood-brain barrier: a cell biological perspective and critical appraisal, Acta Neuropathol 79(2) (1989) 117–28. [PubMed: 2688350]

[96]. Villegas JC, Broadwell RD, Transcytosis of protein through the mammalian cerebral epithelium and endothelium. II. Adsorptive transcytosis of WGA-HRP and the blood-brain and brain-blood barriers, J Neurocytol 22(2) (1993) 67–80. [PubMed: 7680372]

[97]. Banks WA, Fasold MB, Kastin AJ, Measurement of efflux rates from brain to blood, Methods in molecular biology (Clifton, N.J.) 73 (1997) 353–60.

[98]. Banks WA, Kastin AJ, Modulation of the carrier-mediated transport of the Tyr-MIF-1 across the blood-brain barrier by essential amino acids, Journal of Pharmacology and Experimental Therapeutics 239(3) (1986) 668. [PubMed: 2879030]

[99]. Cai HY, Hölscher C, Yue XH, Zhang SX, Wang XH, Qiao F, Yang W, Qi JS, Lixisenatide rescues spatial memory and synaptic plasticity from amyloid β protein-induced impairments in rats, Neuroscience 277 (2014) 6–13. [PubMed: 24583037]

[100]. Zhang H, Meng J, Zhou S, Liu Y, Qu D, Wang L, Li X, Wang N, Luo X, Ma X, Intranasal Delivery of Exendin-4 Confers Neuroprotective Effect Against Cerebral Ischemia in Mice, The AAPS Journal 18(2) (2016) 385–394. [PubMed: 26689204]

[101]. Chauhan MB, Chauhan NB, Brain Uptake of Neurotherapeutics after Intranasal versus Intraperitoneal Delivery in Mice, Journal of neurology and neurosurgery 2(1) (2015) 009. [PubMed: 26366437]

[102]. Banks WA, During MJ, Niehoff ML, Brain Uptake of the Glucagon-Like Peptide-1 Antagonist Exendin(9-39) after Intranasal Administration, Journal of Pharmacology and Experimental Therapeutics 309(2) (2004) 469. [PubMed: 14724226]

[103]. Bosco D, Plastino M, Cristiano D, Colica C, Ermio C, De Bartolo M, Mungari P, Fonte G, Consoli D, Consoli A, Fava A, Dementia is associated with Insulin Resistance in patients with Parkinson's Disease, Journal of the Neurological Sciences 315(1) (2012) 39–43. [PubMed: 22265943]

[104]. Morris JK, Vidoni ED, Honea RA, Burns JM, Impaired glycemia increases disease progression in mild cognitive impairment, Neurobiology of aging 35(3) (2014) 585–589. [PubMed: 24411018]

[105]. Ohara T, Doi Y, Ninomiya T, Hirakawa Y, Hata J, Iwaki T, Kanba S, Kiyohara Y, Glucose tolerance status and risk of dementia in the community: the Hisayama study, Neurology 77 (2011).

[106]. Schrijvers EMC, Witteman JCM, Sijbrands EJG, Hofman A, Koudstaal PJ, Breteler MMB, Insulin metabolism and the risk of Alzheimer disease: The Rotterdam Study, Neurology 75(22) (2010) 1982–1987. [PubMed: 21115952]

[107]. Rönnemaa E, Zethelius B, Sundelöf J, Sundström J, Degerman-Gunnarsson M, Berne C, Lannfelt L, Kilander L, Impaired insulin secretion increases the risk of Alzheimer disease, Neurology 71(14) (2008) 1065–1071. [PubMed: 18401020]

[108]. Hervé F, Ghinea N, Scherrmann JM, CNS delivery via adsorptive transcytosis, Aaps j 10(3) (2008) 455–72. [PubMed: 18726697]

[109]. Villaseñor R, Lampe J, Schwaninger M, Collin L, Intracellular transport and regulation of transcytosis across the blood–brain barrier, Cellular and Molecular Life Sciences 76(6) (2019) 1081–1092. [PubMed: 30523362]

[110]. Villaseñor R, Ozmen L, Messaddeq N, Grüninger F, Loetscher H, Keller A, Betsholtz C, Freskgård PO, Collin L, Trafficking of Endogenous Immunoglobulins by Endothelial Cells at the Blood-Brain Barrier, Sci Rep 6 (2016) 25658. [PubMed: 27149947]

[111]. Hupe-Sodmann K, McGregor GP, Bridenbaugh R, Göke R, Göke B, Thole H, Zimmermann B, Voigt K, Characterisation of the processing by human neutral endopeptidase 24.11 of GLP-1(7-36) amide and comparison of the substrate specificity of the enzyme for other glucagon-like peptides, Regulatory peptides 58(3) (1995) 149–56. [PubMed: 8577927]

[112]. Malm-Erjefält M, Bjørnsdottir I, Vanggaard J, Helleberg H, Larsen U, Oosterhuis B, van Lier JJ, Zdravkovic M, Olsen AK, Metabolism and excretion of the once-daily human glucagon-like peptide-1 analog liraglutide in healthy male subjects and its in vitro degradation by dipeptidyl peptidase IV and neutral endopeptidase, Drug metabolism and disposition: the biological fate of chemicals 38(11) (2010) 1944–53. [PubMed: 20709939]

[113]. Hong WJ, Petell JK, Swank D, Sanford J, Hixson DC, Doyle D, Expression of dipeptidyl peptidase IV in rat tissues is mainly regulated at the mRNA levels, Experimental cell research 182(1) (1989) 256–66. [PubMed: 2565820]

[114]. Iwata N, Takaki Y, Fukami S, Tsubuki S, Saido TC, Region-specific reduction of A beta-degrading endopeptidase, neprilysin, in mouse hippocampus upon aging, J Neurosci Res 70(3) (2002) 493–500. [PubMed: 12391610]

[115]. Willard JR, Barrow BM, Zraika S, Improved glycaemia in high-fat-fed neprilysin-deficient mice is associated with reduced DPP-4 activity and increased active GLP-1 levels, Diabetologia 60(4) (2017) 701–708. [PubMed: 27933334]

[116]. Wright CRA, XLIX.—On the action of organic acids and their anhydrides on the natural alkaloïids. Part I, Journal of the Chemical Society 27(0) (1874) 1031–1043.

[117]. Ward BP, Ottaway NL, Perez-Tilve D, Ma D, Gelfanov VM, Tschöp MH, Dimarchi RD, Peptide lipidation stabilizes structure to enhance biological function, Mol Metab 2(4) (2013) 468–79. [PubMed: 24327962]

[118]. Wang Y, Lomakin A, Kanai S, Alex R, Benedek GB, Transformation of oligomers of lipidated peptide induced by change in pH, Molecular pharmaceutics 12(2) (2015) 411–9. [PubMed: 25569709]

[119]. Kastin AJ, Akerstrom V, Pan W, Interactions of glucagon-like peptide-1 (GLP-1) with the blood-brain barrier, Journal of Molecular Neuroscience 18(1) (2002) 7–14. [PubMed: 11931352]

[120]. Jiang B, Larson JC, Drapala PW, Pérez-Luna VH, Kang-Mieler JJ, Brey EM, Investigation of lysine acrylate containing poly(N-isopropylacrylamide) hydrogels as wound dressings in normal and infected wounds, Journal of biomedical materials research. Part B, Applied biomaterials 100(3) (2012) 668–76. [PubMed: 22121043]

[121]. Banks WA, Kastin AJ, Differential Permeability of the Blood–Brain Barrier to Two Pancreatic Peptides: Insulin and Amylin, Peptides 19(5) (1998) 883–889. [PubMed: 9663454]

[122]. Banks WA, Tschöp M, Robinson SM, Heiman ML, Extent and Direction of Ghrelin Transport Across the Blood-Brain Barrier Is Determined by Its Unique Primary Structure, Journal of Pharmacology and Experimental Therapeutics 302(2) (2002) 822. [PubMed: 12130749]

[123]. Banks WA, Kastin AJ, Huang W, Jaspan JB, Maness LM, Leptin enters the brain by a saturable system independent of insulin, Peptides 17(2) (1996) 305–311. [PubMed: 8801538]

[124]. Rhea EM, Rask-Madsen C, Banks WA, Insulin transport across the blood-brain barrier can occur independently of the insulin receptor, The Journal of physiology 596(19) (2018) 4753–4765. [PubMed: 30044494]

[125]. Ghasemi R, Dargahi L, Haeri A, Moosavi M, Mohamed Z, Ahmadiani A, Brain insulin dysregulation: implication for neurological and neuropsychiatric disorders, Mol Neurobiol 47(3) (2013) 1045–65. [PubMed: 23335160]

[126]. Cantini G, Mannucci E, Luconi M, Perspectives in GLP-1 Research: New Targets, New Receptors, Trends in endocrinology and metabolism: TEM 27(6) (2016) 427–438. [PubMed: 27091492]

[127]. Buhren BA, Gasis M, Thorens B, Müller HW, Bosse F, Glucose-dependent insulinotropic polypeptide (GIP) and its receptor (GIPR): cellular localization, lesion-affected expression, and impaired regenerative axonal growth, J Neurosci Res 87(8) (2009) 1858–70. [PubMed: 19170165]

[128]. Gonzalez-Carter D, Goode AE, Kiryushko D, Masuda S, Hu S, Lopes-Rodrigues R, Dexter DT, Shaffer MSP, Porter AE, Quantification of blood–brain barrier transport and neuronal toxicity of unlabelled multiwalled carbon nanotubes as a function of surface charge, Nanoscale 11(45) (2019) 22054–22069. [PubMed: 31720664]

[129]. Neves-Coelho S, Eleutério RP, Enguita FJ, Neves V, Castanho MARB, A New Noncanonical Anionic Peptide That Translocates a Cellular Blood-Brain Barrier Model, Molecules 22(10) (2017) 1753.

[130]. Raub TJ, Audus KL, Adsorptive endocytosis and membrane recycling by cultured primary bovine brain microvessel endothelial cell monolayers, Journal of Cell Science 97(1) (1990) 127–138. [PubMed: 2258384]

[131]. Banks WA, Characteristics of compounds that cross the blood-brain barrier, BMC Neurology 9(Suppl 1) (2009) S3–S3. [PubMed: 19534732]

[132]. Spranger J, Verma S, Göhring I, Bobbert T, Seifert J, Sindler AL, Pfeiffer A, Hileman SM, Tschöp M, Banks WA, Adiponectin does not cross the blood-brain barrier but modifies cytokine expression of brain endothelial cells, Diabetes 55(1) (2006) 141–7. [PubMed: 16380487]

[133]. Knippenberg S, Thau N, Dengler R, Brinker T, Petri S, Intracerebroventricular injection of encapsulated human mesenchymal cells producing glucagon-like peptide 1 prolongs survival in a mouse model of ALS, PloS one 7(6) (2012) e36857–e36857. [PubMed: 22745655]

[134]. Zhang D, Lv G, Therapeutic potential of spinal GLP-1 receptor signaling, Peptides 101 (2018) 89–94. [PubMed: 29329976]

[135]. Han L, Hölscher C, Xue G-F, Li G, Li D, A novel dual-glucagon-like peptide-1 and glucose-dependent insulinotropic polypeptide receptor agonist is neuroprotective in transient focal cerebral ischemia in the rat, NeuroReport 27(1) (2016) 23–32. [PubMed: 26555034]

[136]. Zhang H, Liu Y, Guan S, Qu D, Wang L, Wang X, Li X, Zhou S, Zhou Y, Wang N, Meng J, Ma X, An Orally Active Allosteric GLP-1 Receptor Agonist Is Neuroprotective in Cellular and Rodent Models of Stroke, PloS one 11(2) (2016) e0148827–e0148827. [PubMed: 26863436]

[137]. Barkas F, Elisaf M, Milionis H, Protection against stroke with glucagon-like peptide 1 receptor agonists: a systematic review and meta-analysis, European journal of neurology 26(4) (2019) 559–565. [PubMed: 30629331]

[138]. Shan Y, Tan S, Lin Y, Liao S, Zhang B, Chen X, Wang J, Deng Z, Zeng Q, Zhang L, Wang Y, Hu X, Qiu W, Peng L, Lu Z, The glucagon-like peptide-1 receptor agonist reduces inflammation and blood-brain barrier breakdown in an astrocyte-dependent manner in experimental stroke, Journal of Neuroinflammation 16(1) (2019) 242. [PubMed: 31779652]

[139]. Yang X, Feng P, Zhang X, Li D, Wang R, Ji C, Li G, Hölscher C, The diabetes drug semaglutide reduces infarct size, inflammation, and apoptosis, and normalizes neurogenesis in a rat model of stroke, Neuropharmacology 158 (2019) 107748. [PubMed: 31465784]

[140]. Marsico F, Paolillo S, Gargiulo P, Bruzzese D, Dell'Aversana S, Esposito I, Renga F, Esposito L, Marciano C, Dellegrottaglie S, Iesu I, Perrone Filardi P, Effects of glucagon-like peptide-1 receptor agonists on major cardiovascular events in patients with Type 2 diabetes mellitus with or without established cardiovascular disease: a meta-analysis of randomized controlled trials, European Heart Journal (2020).

[141]. Glotfelty EJ, Delgado TE, Tovar-y-Romo LB, Luo Y, Hoffer BJ, Olson L, Karlsson TE, Mattson MP, Harvey BK, Tweedie D, Li Y, Greig NH, Incretin Mimetics as Rational Candidates for the Treatment of Traumatic Brain Injury, ACS Pharmacology & Translational Science 2(2) (2019) 66–91. [PubMed: 31396586]

[142]. Rakipovski G, Rolin B, Nøhr J, Klewe I, Frederiksen KS, Augustin R, Hecksher-Sørensen J, Ingvorsen C, Polex-Wolf J, Knudsen LB, The GLP-1 Analogs Liraglutide and Semaglutide Reduce Atherosclerosis in ApoE(−/−) and LDLr(−/−) Mice by a Mechanism That Includes Inflammatory Pathways, JACC. Basic to translational science 3(6) (2018) 844–857. [PubMed: 30623143]

[143]. Rizzo M, Nikolic D, Patti AM, Mannina C, Montalto G, McAdams BS, Rizvi AA, Cosentino F, GLP-1 receptor agonists and reduction of cardiometabolic risk: Potential underlying mechanisms, Biochimica et biophysica acta. Molecular basis of disease 1864(9 Pt B) (2018) 2814–2821. [PubMed: 29778663]

[144]. Hakon J, Ruscher K, Romner B, Tomasevic G, Preservation of the Blood Brain Barrier and Cortical Neuronal Tissue by Liraglutide, a Long Acting Glucagon-Like-1 Analogue, after Experimental Traumatic Brain Injury, PLoS ONE 10(3) (2015) e0120074. [PubMed: 25822252]

[145]. Zhao L, Li Z, Vong JSL, Chen X, Lai H-M, Yan LYC, Huang J, Sy SKH, Tian X, Huang Y, Chan HYE, So H-C, Ng W-L, Tang Y, Lin W-J, Mok VCT, Ko H, Zonation-dependent single-endothelial cell transcriptomic changes in the aged brain, bioRxiv (2019)800318.

[146]. Hamilton A, Patterson S, Porter D, Gault VA, Holscher C, Novel GLP-1 mimetics developed to treat type 2 diabetes promote progenitor cell proliferation in the brain, J Neurosci Res 89 (2011).

[147]. Isacson R, Nielsen E, Dannaeus K, Bertilsson G, Patrone C, Zachrisson O, Wikström L, The glucagon-like peptide 1 receptor agonist exendin-4 improves reference memory performance and decreases immobility in the forced swim test, European Journal of Pharmacology 650(1) (2011) 249–255. [PubMed: 20951130]

[148]. Faivre E, Hamilton A, Hölscher C, Effects of acute and chronic administration of GIP analogues on cognition, synaptic plasticity and neurogenesis in mice, European Journal of Pharmacology 674(2) (2012) 294–306. [PubMed: 22115896]

[149]. Lennox R, Porter DW, Flatt PR, Gault VA, (Val8)GLP-1-Glu-PAL: a GLP-1 Agonist That Improves Hippocampal Neurogenesis, Glucose Homeostasis, and β-Cell Function in High-Fat-Fed Mice, ChemMedChem 8(4) (2012) 595–602. [PubMed: 23138973]

[150]. Parthsarathy V, Hölscher C, Chronic Treatment with the GLP1 Analogue Liraglutide Increases Cell Proliferation and Differentiation into Neurons in an AD Mouse Model, PLoS ONE 8(3) (2013) e58784. [PubMed: 23536825]

[151]. Yang J-L, Chen W-Y, Chen S-D, The Emerging Role of GLP-1 Receptors in DNA Repair: Implications in Neurological Disorders, International journal of molecular sciences 18(9) (2017) 1861.

[152]. Bomba M, Granzotto A, Castelli V, Massetti N, Silvestri E, Canzoniero LMT, Cimini A, Sensi SL, Exenatide exerts cognitive effects by modulating the BDNF-TrkB neurotrophic axis in adult mice, Neurobiol Aging 64 (2018) 33–43. [PubMed: 29331730]

[153]. Park SW, Mansur RB, Lee Y, Lee J-H, Seo MK, Choi AJ, McIntyre RS, Lee JG, Liraglutide Activates mTORC1 Signaling and AMPA Receptors in Rat Hippocampal Neurons Linder Toxic Conditions, Frontiers in neuroscience 12(756) (2018).

[154]. Gengler S, McClean PL, McCurtin R, Gault VA, Hölscher C, Val(8)GLP-1 rescues synaptic plasticity and reduces dense core plaques in APP/PS1 mice, Neurobiology of Aging 33(2) (2012) 265–276. [PubMed: 20359773]

[155]. Duffy AM, Hölscher C, The incretin analogue D-Ala2GIP reduces plaque load, astrogliosis and oxidative stress in an APP/PS1 mouse model of Alzheimer's disease, Neuroscience 228 (2013) 294–300. [PubMed: 23103794]

[156]. Faivre E, Hölscher C, Neuroprotective effects of D-Ala(2)GIP on Alzheimer's disease biomarkers in an APP/PS1 mouse model, Alzheimer's Research & Therapy 5(2) (2013) 20–20.

[157]. Faivre E, Hölscher C, D-Ala2GIP facilitated synaptic plasticity and reduces plaque load in aged wild type mice and in an Alzheimer's disease mouse model, J Alzheimers Dis 35(2) (2013) 267–83. [PubMed: 23568101]

[158]. Gault VA, Hölscher C, GLP-1 agonists facilitate hippocampal LTP and reverse the impairment of LTP induced by beta-amyloid, European Journal of Pharmacology 587(1) (2008) 112–117. [PubMed: 18466898]

[159]. Gault VA, Hölscher C, Protease-Resistant Glucose-Dependent Insulinotropic Polypeptide Agonists Facilitate Hippocampal LTP and Reverse the Impairment of LTP Induced by Beta-Amyloid, Journal of Neurophysiology 99(4) (2008) 1590–1595. [PubMed: 18234983]

[160]. Wang XH, Li L, Holscher C, Pan YF, Chen XR, Qi JS, Val8-glucagon-like peptide-1 protects against Abeta1-40-induced impairment of hippocampal late-phase long-term potentiation and spatial learning in rats, Neuroscience 170 (2010).

[161]. Han W-N, Hölscher C, Yuan L, Yang W, Wang X-H, Wu M-N, Qi J-S, Liraglutide protects against amyloid-β protein-induced impairment of spatial learning and memory in rats, Neurobiology of Aging 34(2) (2013) 576–588. [PubMed: 22592020]

[162]. Wang XH, Yang W, Hölscher C, Wang ZJ, Cai HY, Li QS, Qi JS, Val^{8}-GLP-1 remodels synaptic activity and intracellular calcium homeostasis impaired by amyloid β peptide in rats, J Neurosci Res 91(4) (2013) 568–77. [PubMed: 23335292]

[163]. Chen S, An F.m., Yin L, Liu A.r., Yin D.k., Yao W.b., Gao X.d., Glucagon-like peptide-1 protects hippocampal neurons against advanced glycation end product-induced tau hyperphosphorylation, Neuroscience 256 (2014) 137–146. [PubMed: 24183963]

[164]. Zhang H, Meng J, Li X, Zhou S, Qu D, Wang N, Jia M, Ma X, Luo X, Pro-GLP-1, a Pro-drug of GLP-1, is neuroprotective in cerebral ischemia, European Journal of Pharmaceutical Sciences 70 (2015) 82–91. [PubMed: 25640912]

[165]. Briyal S, Shah S, Gulati A, Neuroprotective and anti-apoptotic effects of liraglutide in the rat brain following focal cerebral ischemia, Neuroscience 281 (2014) 269–281. [PubMed: 25301749]

[166]. Zhang Y, Chen Y, Li L, Hölscher C, Neuroprotective effects of (Val8)GLP-1-Glu-PAL in the MPTP Parkinson's disease mouse model, Behavioural Brain Research 293 (2015) 107–113. [PubMed: 26187689]

[167]. Sharma MK, Jalewa J, Hölscher C, Neuroprotective and anti-apoptotic effects of liraglutide on SH-SY5Y cells exposed to methylglyoxal stress, J Neurochem 128(3) (2014) 459–71. [PubMed: 24112036]

[168]. During MJ, Cao L, Zuzga DS, Francis JS, Fitzsimons HL, Jiao X, Bland RJ, Klugmann M, Banks WA, Drucker DJ, Haile CN, Glucagon-like peptide-1 receptor is involved in learning and neuroprotection, Nature Medicine 9 (2003) 1173.

[169]. Eakin K, Li Y, Chiang Y-H, Hoffer BJ, Rosenheim H, Greig NH, Miller JP, Exendin-4 Ameliorates Traumatic Brain Injury-Induced Cognitive Impairment in Rats, PLOS ONE 8(12) (2013) e82016. [PubMed: 24312624]

[170]. Perry T, Haughey NJ, Mattson MP, Egan JM, Greig NH, Protection and reversal of excitotoxic neuronal damage by glucagon-like peptide-1 and exendin-4, The Journal of pharmacology and experimental therapeutics 302(3) (2002) 881–8. [PubMed: 12183643]

[171]. Gilman CP, Perry T, Furukawa K, Grieg NH, Egan JM, Mattson MP, Glucagon-like peptide 1 modulates calcium responses to glutamate and membrane depolarization in hippocampal neurons, J Neurochem 87(5) (2003) 1137–44. [PubMed: 14622093]

[172]. Yu Y-W, Hsieh T-H, Chen K-Y, Wu JC-C, Hoffer BJ, Greig NH, Li Y, Lai J-H, Chang C-F, Lin J-W, Chen Y-H, Yang L-Y, Chiang Y-H, Glucose-Dependent Insulinotropic Polypeptide Ameliorates Mild Traumatic Brain Injury-Induced Cognitive and Sensorimotor Deficits and Neuroinflammation in Rats, Journal of Neurotrauma 33(22) (2016) 2044–2054. [PubMed: 26972789]

[173]. Oh YS, Jun H-S, Effects of Glucagon-Like Peptide-1 on Oxidative Stress and Nrf2 Signaling, International journal of molecular sciences 19(1) (2017) 26.

[174]. Abbas T, Faivre E, Hölscher C, Impairment of synaptic plasticity and memory formation in GLP-1 receptor KO mice: Interaction between type 2 diabetes and Alzheimer's disease, Behavioural Brain Research 205(1) (2009) 265–271. [PubMed: 19573562]

[175]. Gault VA, Porter WD, Flatt PR, Hölscher C, Actions of exendin-4 therapy on cognitive function and hippocampal synaptic plasticity in mice fed a high-fat diet, International Journal Of Obesity 34 (2010) 1341. [PubMed: 20351729]

[176]. McClean PL, Gault VA, Harriott P, Hölscher C, Glucagon-like peptide-1 analogues enhance synaptic plasticity in the brain: A link between diabetes and Alzheimer's disease, European Journal of Pharmacology 630(1) (2010) 158–162. [PubMed: 20035739]

[177]. Faivre E, Gault VA, Thorens B, Hölscher C, Glucose-dependent insulinotropic polypeptide receptor knockout mice are impaired in learning, synaptic plasticity, and neurogenesis, Journal of Neurophysiology 105(4) (2011) 1574–1580. [PubMed: 21273318]

[178]. Porter DW, Irwin N, Flatt PR, Hölscher C, Gault VA, Prolonged GIP receptor activation improves cognitive function, hippocampal synaptic plasticity and glucose homeostasis in high-fat fed mice, European Journal of Pharmacology 650(2) (2011) 688–693. [PubMed: 21050845]

[179]. Porter DW, Kerr BD, Flatt PR, Holscher C, Gault VA, Four weeks administration of Liraglutide improves memory and learning as well as glycaemic control in mice with high fat dietary-induced obesity and insulin resistance, Diabetes, Obesity and Metabolism 12(10) (2010) 891–899.

[180]. Porter WD, Flatt PR, Hölscher C, Gault VA, Liraglutide improves hippocampal synaptic plasticity associated with increased expression of Mash1 in ob/ob mice, International Journal Of Obesity 37 (2012) 678. [PubMed: 22665137]

[181]. Ma T, Du X, Pick JE, Sui G, Brownlee M, Klann E, Glucagon-like Peptide-1 Cleavage Product GLP-1 (9-36) Amide Rescues Synaptic Plasticity and Memory Deficits in Alzheimer’s Disease Model Mice, The Journal of neuroscience : the official journal of the Society for Neuroscience 32(40) (2012) 13701–13708. [PubMed: 23035082]

[182]. Iwai T, Sawabe T, Tanimitsu K, Suzuki M, Sasaki-Hamada S, Oka J-I, Glucagon-like peptide-1 protects synaptic and learning functions from neuroinflammation in rodents, Journal of Neuroscience Research 92(4) (2014) 446–454. [PubMed: 24464856]

[183]. Lennox R, Flatt PR, Gault VA, Lixisenatide improves recognition memory and exerts neuroprotective actions in high-fat fed mice, Peptides 61 (2014) 38–47. [PubMed: 25195184]

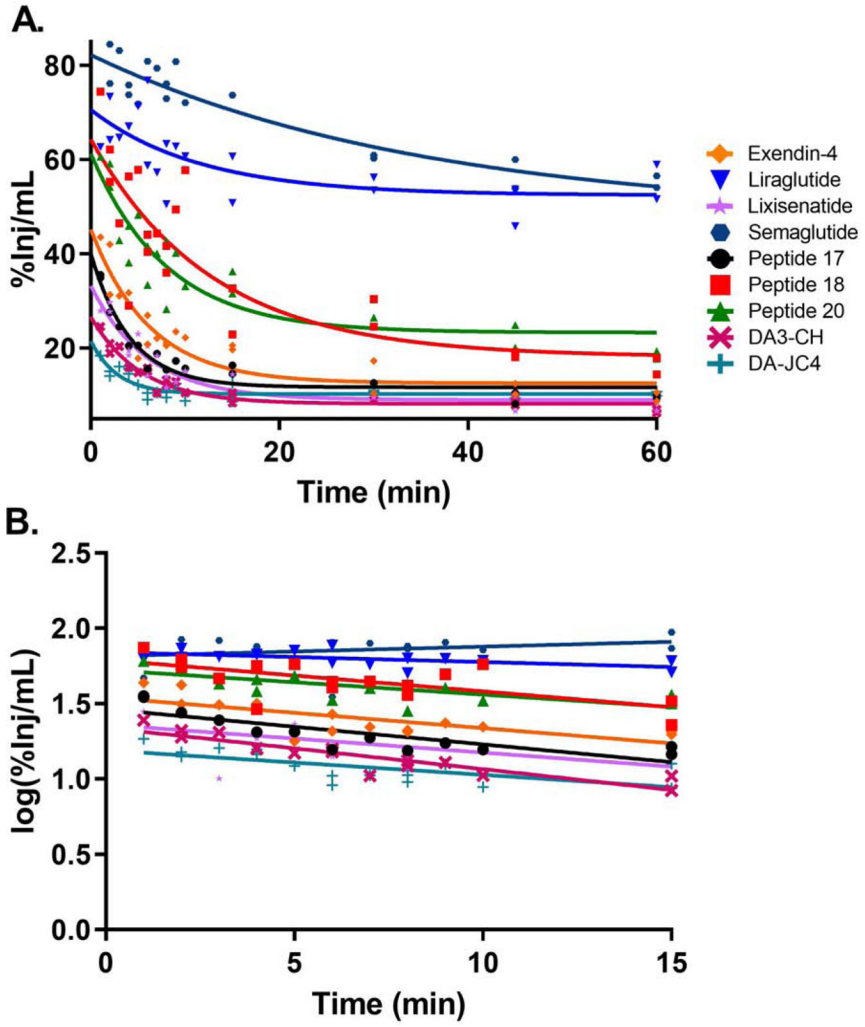

Fig 1.

Clearance of ^{125}I-IRAs from serum. The level of radioactivity in serum over 60 min clock time is graphed in (A). The linear distribution phase during the first 15 min when represented as log(%Inj/mL) was used to calculate the clearance (B). The half-time clearance from blood for each IRA is listed in Table 3.

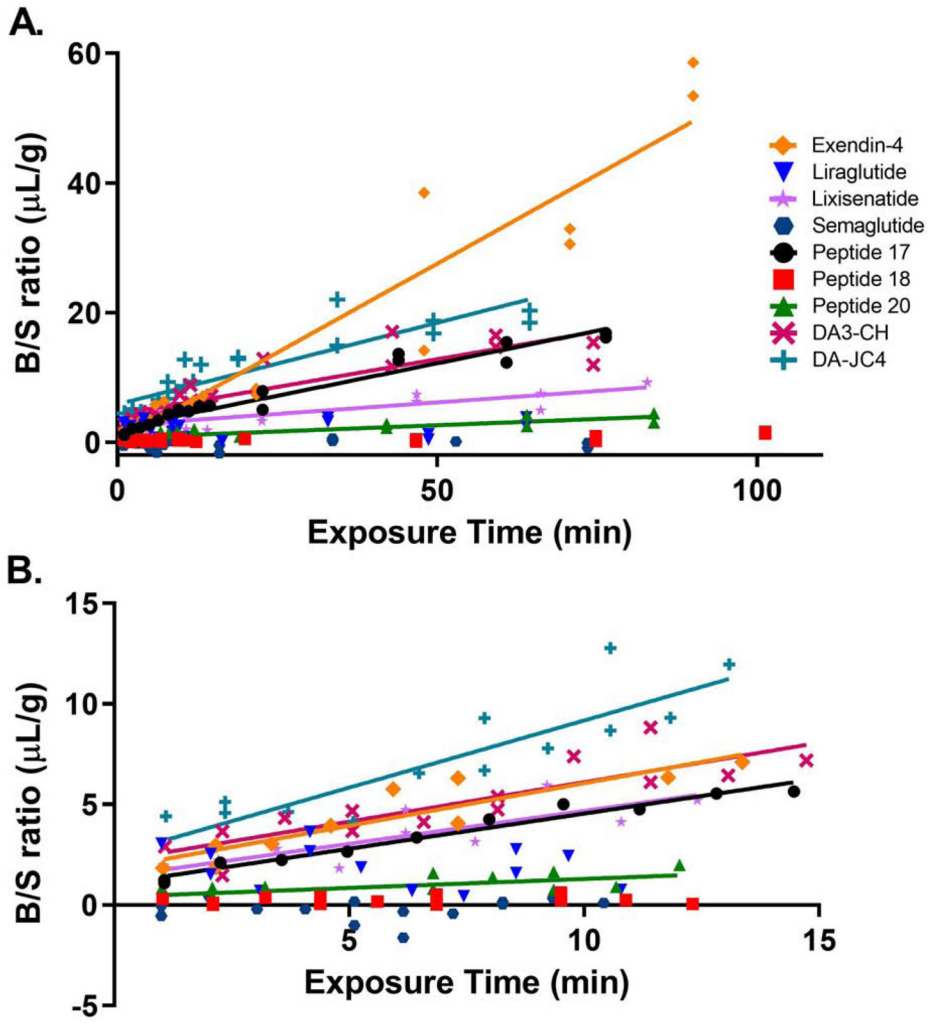

Fig. 2.

Multiple-time regression analysis of ^{125}I-IRAs across the BBB. The brain to serum (B/S) ratios of radioactivity, corrected for vascular space, present in whole brain over the entire time curve are graphed in (A). The linear first 10 min clock time of the experiments are shown in (B) and are used to calculate the unidirectional influx rate, K_i for Fig. 3 and Table 3.

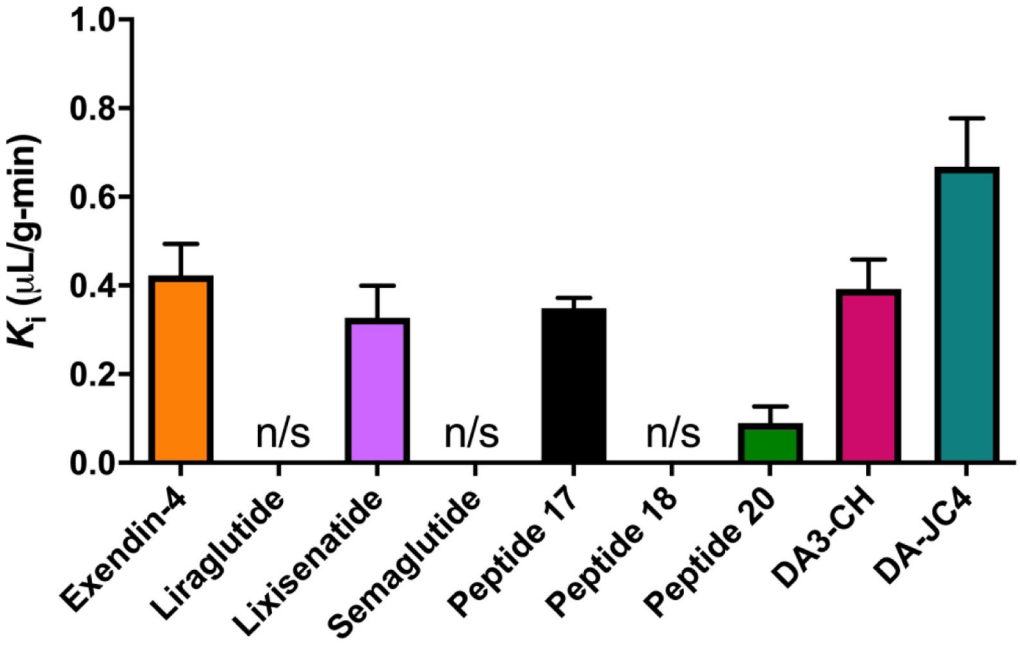

Fig. 3.

Rate constants of ^{125}I-IRAs transport into whole brain. The unidirectional influx rates, K_i (slope) and V_i (y-intercept) are listed in Table 3. n=10-14/IRA

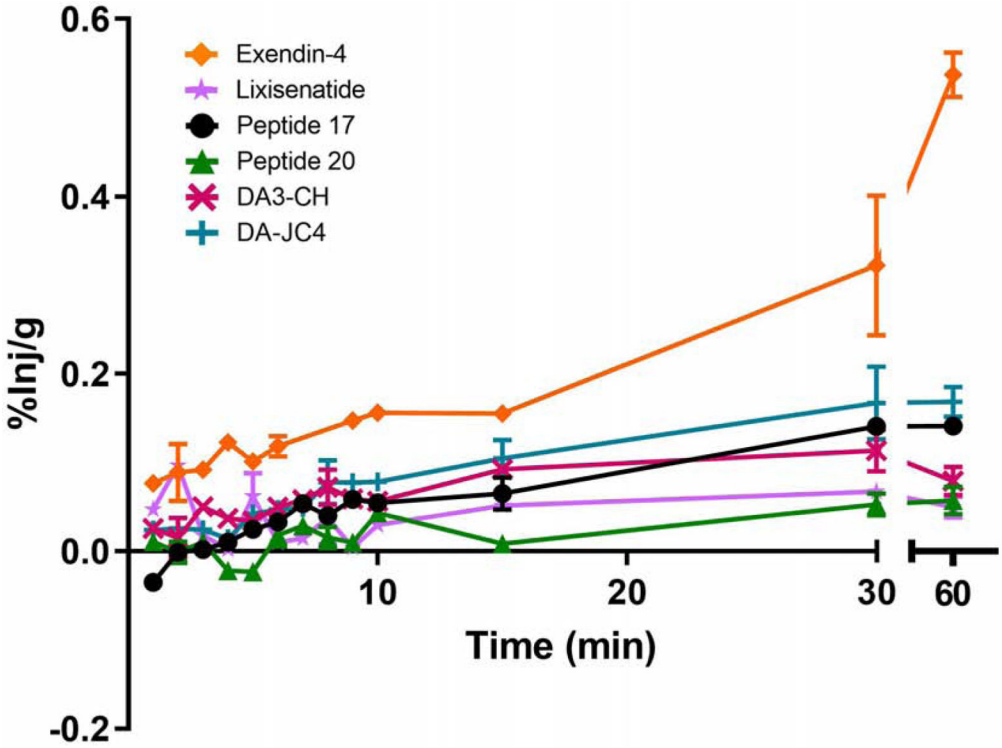

Fig. 4.

Percent of the iv injected dose of ^{125}I-IRAs taken up per gram of brain tissue (%Inj/g) corrected for the initial level of vascular binding (V_i). The values for all the tested IRAs other than exendin-4 plateaued by 30 min. n=1-2/time point/IRA

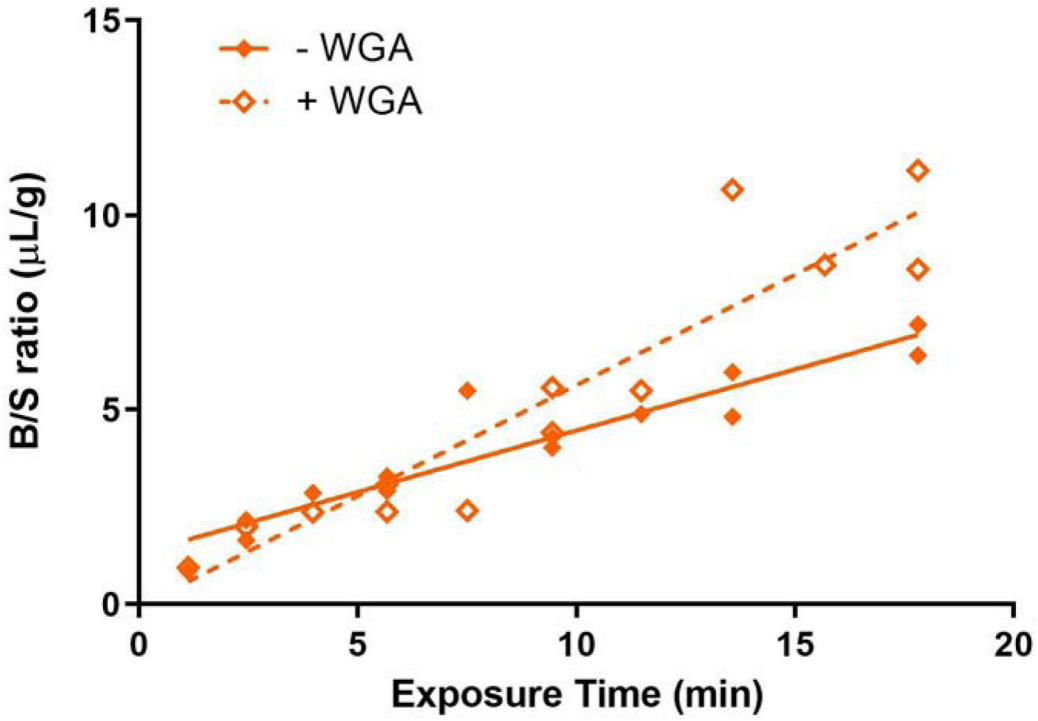

Fig. 5.

Characterization of exendin-4 influx into brain. The influx of ^{125}I-exendin-4 was enhanced by WGA about 45% in the time span of the study. Results are expressed in terms of tissue to serum (T/S) ratios.

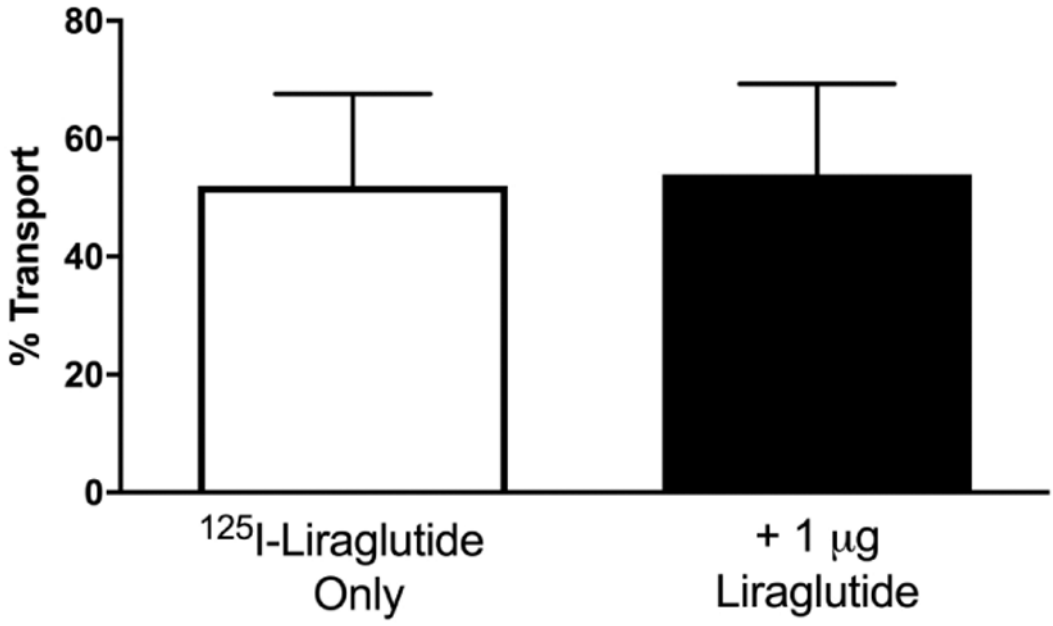

Fig. 6.

Characterization of liraglutide efflux from brain. Brain-to-blood efflux of ^{125}I-liraglutide was not inhibited by 1 μg unlabeled liraglutide, consistent with a non-saturable efflux mechanism. Results are expressed as % Transport defined in section 2.12. Data are presented as mean ± SEM with n = 10 per group.

Table 1.

Characteristics of IRA Peptides Studied

Peptide	Description[a]	Sequence (and Amino Acid Number)[b]	MW[c]	Charge[d]	Hydrophobic amino acids	Lipid Solubility Partition Coefficient	Log Partition Coefficient (Log P)
Single IRAs:							
Exendin-4	Synthetic exendin-4 (endogenous lizard GLP-1 mimetic)	HGEGTFTSDLSKQMEEEAVRLFIEWLKNGGPSSGAPPPS-NH2 (39 aa)	4187	−2.0	41%	0.0031 ± 0.0009	−2.522 ± 0.1476
Liraglutide	Acylated hGLP-1 (7-37) analogue	HAEGTFTSDVSSYLEGQAAK[a]EFIAWLVRGRG-OH (31 aa)	3751	−0.9	35%	0.0123 ± 0.0008	−1.910 ± 0.0288
Lixisenatide	Non-acylated GLP-1 (7-37) analogue based on exendin-4	HGEGTFTSDLSKQMEEEAVRLFIEWLKNGGPSSGAPPSKKKKKK-NH2 (44 aa)	4858	4.1	50%	0.0021 ± 0.0003	−2.683 ± 0.0717
Semaglutide	Acylated hGLP-1 (7-37) analogue	HXEGTFTSDVSSYLEGQAAK[b]EFIAWLVRGRG-OH (31 aa)	4113	−0.9	37%	0.0353 ± 0.0016	−1.452 ± 0.0199
Dual IRAs (DAs):							
Native DA (Peptide 17)	hGLP-1R/GIPR agonist = peptide 17 of Finan and Ma et al. [87]	YXEGTFTSDYSIYLDKQAAXEFVNWLLAGGPSSGAPPPSC-NH2 (40 aa)	4473	−2.0	32%	0.0052 ± 0.0049	−2.564 ± 0.5921
Acylated DA (Peptide 18)	Acylated hGLP-1R/GIPR agonist = peptide 18 of Finan and Ma et al. [87]	YXEGTFTSDYSIYLDKQAAXEFVNWLLAGGPSSGAPPPSK-NH2 (40 aa)	4865	−1.0	34%	0.2493 ± 0.0239 *	−0.604 ± 0.0418 *
PEGylated DA (Peptide 20)	PEGylated hGLP-1R/ GIPR agonist = peptide 20 of Finan and Ma et al. [87]	YXEGTFTSDYSIYLDKQAAXEFVC *WLLAGGPSSGAPPPSK-NH2 (40 aa)	44,473	−1.0	34%	0.0057 ± 0.0008	−2.249 ± 0.0671
DA3-CH	hGLP-1R/GIPR agonist = Finan and Ma et al. peptide 17 [87] with substitution of terminal lysine for cysteine	YXEGTFTSDYSIYLDKQAAXEFVNWLLAGGPSSGAPPPSK-NH2 (40 aa)	4448	−1.0	34%	0.0048 ± 0.0015	−2.325 ± 0.1318
DA-JC4	hGLP-1R/GIPR agonist = Finan and Ma et al. [87] peptide 17 with terminal cysteine replaced by 6 lysines	YXEGTFTSDYSIYLDKQAAXEFVNWLLAGGPSSGAPPPSKKKKKK-NH2 (45 aa)	5620	4.0	44%	0.0030 ± 0.0008	−2.520 ± 0.1184

[a] hGLP-1R = human glucagon-like peptide 1 receptor; hGLP-1R/GIPR = human GLP-1R + human glucose dependent insulinotropic polypeptide (GIP) receptor

[b] Sequences for all peptides except lixisenatide and semaglutide are from Suppl. Fig. 1 in Finan and Ma et al. [87]. C* in Peptide 20 = cysteine linked to a 40 kDa polyethylene glycol (PEG) group. K^a in liraglutide = lysine linked via glutamate to a C16 acyl group. K^b in semaglutide = lysine linked via glutamate to a C18-diacid acyl group. X in semaglutide and dual IRAs = aminoisobutyric acid.

[c] Molecular weight (g/mol = Da).

[d] Net charge at pH 7 was determined using calculator at http://www.bachem.com/service-support/peptide-calculator/

* $p < 0.05$ compared to lipid solubility of all other IRAs tested

Table 2.

In Vivo Degradation of ^{125}I-IRA Peptides*

Peptide	Whole Brain			Serum		
	10 min	60 min	PC	10 min	60 min	PC
Single IRAs:						
Exendin-4	79.04 ± 2.750	37.71 ± 5.330[a]	68.1 ± 1.3	93.58 ± 1.440	76.45 ± 6.580	87.9 ± 0.8
Liraglutide	100.1 ± 4.206	88.81 ± 10.15[a]	85.4 ± 3.7	101.2 ± 0.062	100.18 ± 0.244[a]	97.4
Lixisenatide	83.91 ± 10.00	78.13 ± 5.167	72.9 ± 0.4	97.57 ± 0.430	80.10 ± 1.607[a]	87.4 ± 0.7
Semaglutide	95.55 ± 1.139	90.44 ± 2.026[a]	99.4 ± 0.0	100.0 ± 0.031	98.91 ± 0.029[a]	99.8 ± 0.0
Dual IRAs:						
Peptide 17	78.98 ± 3.930	52.91 ± 5.030[a]	94.3 ± 0.2	95.77 ± 0.350	81.20 ± 1.960[a]	98.6 ± 0.0
Peptide 18	107.8 ± 3.37	78.48 ± 4.120[a]	91.2 ± 1.0	99.85 ± 0.020	90.78 ± 4.440	99.1 ± 0.2
Peptide 20	99.4 ± 2.070	75.20 ± 5.101[a]	92.9 ± 1.2	100.16 ± 0.120	93.80 ± 1.850[a]	98.2 ± 0.1
DA3-CH	71.59 ± 12.14	26.71 ± 17.23[a]	76.0 ± 2.0	93.26 ± 1.110	73.65 ± 3.138[a]	97.6 ± 0.1
DA-JC4	69.63 ± 16.36	47.99 ± 18.71	72.1 ± 1.0	85.66 ± 1.866	63.32 ± 1.987[a]	88.7 ± 0.8

*The data shown are mean ± SEM percentages of ^{125}I-labelled IRAs injected iv that remained intact 10 or 60 min later as reflected in accumulation of radioactive degradation products with time as determined by precipitation of those products. Data are expressed relative to processing controls (PC, n = 1-2) with n = 3 per group.

[a]$p<0.05$ vs values at 10 min post injection.

Table 3.

Pharmacokinetics of ^{125}I-IRA Peptides

Peptide	Half-Time Serum Clearance	Blood to Brain Influx			Initial Volume of Distribution in Brain	Capillary Depletion		
	$t_{1/2}$ (min)	K*i* (μL/g-min)	r with time*	p	V*i* (μL/g)	Capillary	Parenchyma	%Parenchyma
Single IRAs:								
Exendin-4	33.44	0.4231±0.0703	0.8191	0.0003	1.824 ± 0.4987	1.255 ± 0.448	6.693 ± 1.532	84.2
Liraglutide	167.22	ns	0.1006	0.2691	2.434 ± 0.5977	1.103 ± 0.153	0.444 ± 0.315	28.7
Lixisenatide	37.66	0.3271±0.0726	0.6924	0.0015	1.409 ± 0.5059	1.182 ± 0.161	2.383 ± 0.290	66.8
Semaglutide	149.31	ns	0.0137	0.6893	−0.340 ± 0.3285	0.434 ± 0.056	−0.850 ± 0.533	0
Dual IRAs:								
Peptide 17	39.61	0.3489±0.0228	0.9627	<0.0001	1.057 ± 0.1876	0.543 ± 0.178	1.482 ± 0.462	73.2
Peptide 18	32.37	ns	0.0151	0.689	0.2034 ± 0.1134	0.764 ± 0.092	−0.306 ± 0.219	0
Peptide 20	43	0.0892±0.0382	0.3307	0.0398	0.4075 ± 0.2728	0.796 ± 0.252	0.615 ± 0.807	43.6
DA3-CH	42.57	0.3922±0.0668	0.7418	<0.0001	2.186 ± 0.5638	0.637 ± 0.073	3.918 ± 0.993	86.02
DA-JC4	151.94	0.6680±0.1089	0.7582	<0.0001	2.495 ± 0.8554	1.129 ± 0.597	9.855 ±2.751	89.7

Table 4.

Saturability of ^{125}I-IRA Peptide Transport into Brain*

Peptide	Whole Brain		Serum	
	Without Unlabeled IRA	With Unlabeled IRA	Without Unlabeled IRA	With Unlabeled IRA
Single IRAs:				
Exendin-4	17.32 ± 1.422	18.67 ± 1.365	110.0 ± 9.812	109.1 ± 9.753
Liraglutide	8.02 ± 0.549	9.86 ± 0.631[a]	573.1 ± 21.03	447.8 ± 13.50[a]
Lixisenatide	14.78 ± 0.724	13.51 ± 0.743	40.90 ± 2.027	48.21 ± 4.246
Semaglutide	9.637 ± 0.308	9.430 ± 0.344	692.1 ± 55.27	723.6 ± 41.74
Dual IRAs:				
Peptide 17	11.41 ± 0.528	11.34 ± 0.321	81.33 ± 6.720	89.47 ± 5.466
Peptide 18	7.18 ± 0.202	7.43 ± 0.265	422.7 ± 26.50	349.4 ± 20.50[a]
Peptide 20	9.51 ± 0.421	9.56 ± 0.287	217.3 ± 7.176	216.2 ± 5.307
DA3-CH	20.86 ± 1.943	19.44 ± 0.866	65.07 ± 6.275	63.13 ± 3.087
DA-JC4	15.10 ± 1.243	17.10 ± 3.232	29.32 ± 2.014	31.07 ± 2.426

*Values are mean ± SEM (μL/g) of brain/serum ratios (n = 5-16 per group). Data were analyzed by a two-tailed, unpaired t test

[a]$p < 0.05$ comparing samples with or without unlabeled IRA peptides.